USGS
science for a changing world

Prepared in cooperation with the
GRAND CANYON MONITORING AND RESEARCH CENTER

Modeling Water-Surface Elevations and Virtual Shorelines for the Colorado River in Grand Canyon, Arizona

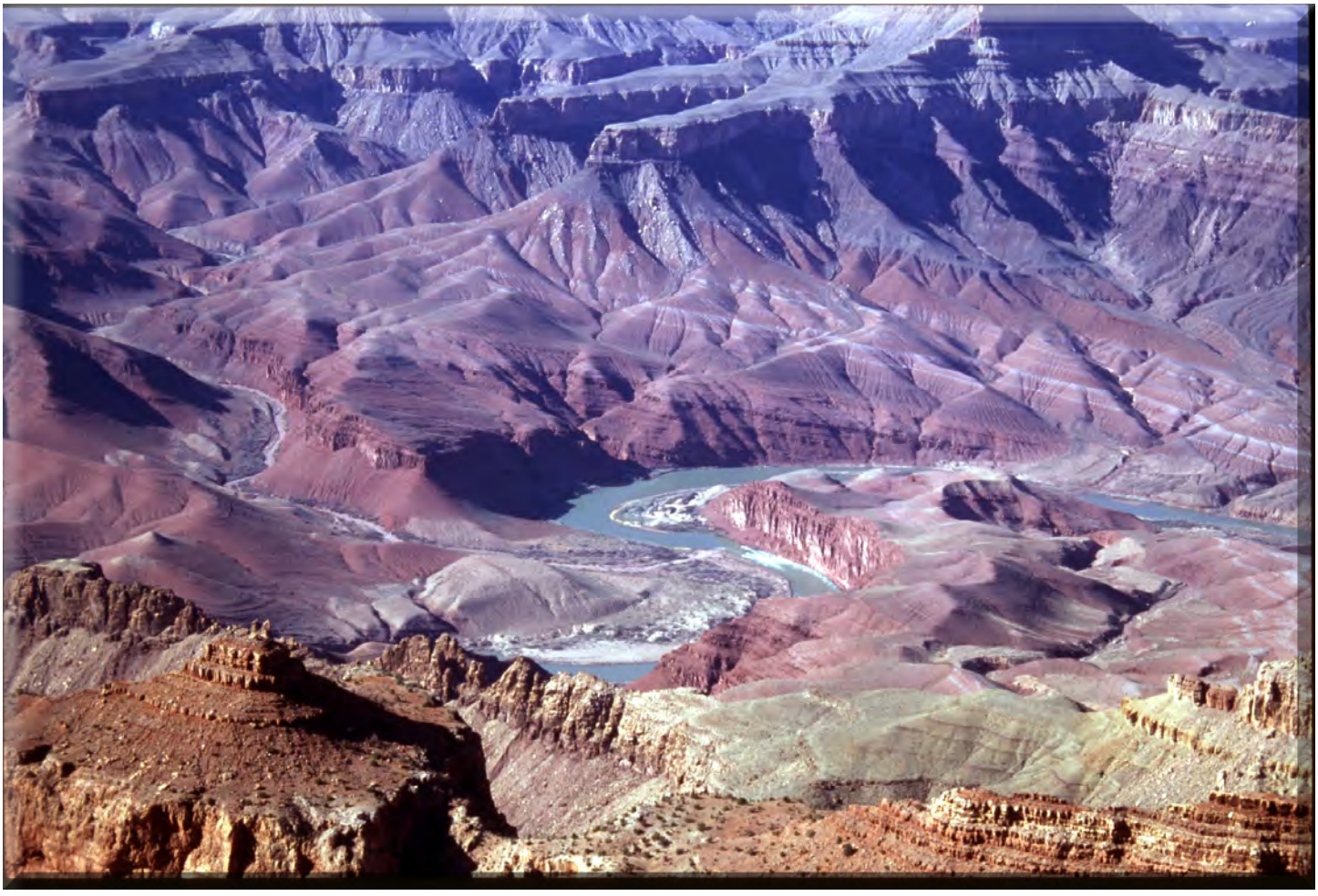

Scientific Investigation Report 2008–5075

U.S. Department of the Interior
U.S. Geological Survey

Cover Photo: Colorado River and the Unkar Delta from Lipan Point, Grand Canyon National Park, Arizona, by C.S. Magirl in 2003.

Modeling Water-Surface Elevations and Virtual Shorelines for the Colorado River in Grand Canyon, Arizona

By Christopher S. Magirl, Michael J. Breedlove, Robert H. Webb, and Peter G. Griffiths

Prepared in cooperation with the
GRAND CANYON MONITORING AND RESEARCH CENTER

Scientific Investigation Report 2008-5075

U.S. Department of the Interior
U.S. Geological Survey

U.S. Department of the Interior
DIRK KEMPTHORNE, Secretary

U.S. Geological Survey
Robert D. Meyers, Director

U.S. Geological Survey, Reston, Virginia: 2008

For product and ordering information:
World Wide Web: http://www.usgs.gov/pubprod
Telephone: 1-888-ASK-USGS

For more information on the USGS--the Federal source for science about the Earth, its natural and living resources, natural hazards, and the environment:
World Wide Web: http://www.usgs.gov
Telephone: 1-888-ASK-USGS

Suggested citation:
Magirl. Christopher, F.N., Webb Robert, Griffiths Peter, 2008, Modeling Water-Surface Elevations and Virtual Shorelines for the Colorado River in Grand Canyon, Arizona, U.S.Geological Survey Scientific Investigations Report 2008-5075, 32p

Contents

Figures

Tables

Multiply	By	To obtain
	Length	
foot (ft)	0.3048	meter (m)
mile (mi)	1.609	kilometer (km)
	Volume	
cubic foot (ft^3)	0.02832	cubic meter (m^3)
cubic yard (yd^3)	0.7646	cubic meter (m^3)
	Flow rate	
cubic foot per second (ft^3/s)	0.02832	cubic meter per second (m^3/s)
cubic foot per second per square mile [$(ft^3/s)/mi^2$]	0.01093	cubic meter per second per square kilometer [$(m^3/s)/km^2$]
cubic foot per day (ft^3/d)	0.02832	cubic meter per day (m^3/d)

Vertical coordinate information is referenced in meters to height above the GRS80 ellipse defined by NAD83(1992).

Horizontal coordinate information is referenced to North American Datum of 1983, NAD83(1992).

Elevation, as used in this report, refers to distance above the vertical datum.

Abbreviations and Acronyms

AML	Arc Macro Language
DEM	Digital Elevation Model
GCMRC	Grand Canyon Monitoring and Research Center
GIS	Geographic Information System
GUI	Graphic User Interface
HEC	Hydraulic Engineering Center
ISP	Integrated Science Program
LIDAR	Light Detection and Ranging
LOB	Left overbank
NAU	Northern Arizona University
RAS	River Analysis System
ROB	Right overbank
STARS	Sediment Transport and River Simulation
USGS	United States Geological Survey
WSPRO	Water Surface Profile

Modeling Water-Surface Elevations and Virtual Shorelines for the Colorado River in Grand Canyon, Arizona

By Christopher S. Magirl, Michael J. Breedlove, Robert H. Webb, and Peter G. Griffiths

Abstract

Using widely-available software intended for modeling rivers, a new one-dimensional hydraulic model was developed for the Colorado River through Grand Canyon from Lees Ferry to Diamond Creek. Solving one-dimensional equations of energy and continuity, the model predicts stage for a known steady-state discharge at specific locations, or cross sections, along the river corridor. This model uses 2,680 cross sections built with high-resolution digital topography of ground locations away from the river flowing at a discharge of 227 m^3/s; synthetic bathymetry was created for topography submerged below the 227 m^3/s water surface. The synthetic bathymetry was created by adjusting the water depth at each cross section up or down until the model's predicted water-surface elevation closely matched a known water surface. This approach is unorthodox and offers a technique to construct one-dimensional hydraulic models of bedrock-controlled rivers where bathymetric data have not been collected. An analysis of this modeling approach shows that while effective in enabling a useful model, the synthetic bathymetry can differ from the actual bathymetry. The known water-surface profile was measured using elevation data collected in 2000 and 2002, and the model can simulate discharges up to 5,900 m^3/s. In addition to the hydraulic model, GIS-based techniques were used to estimate virtual shorelines and construct inundation maps.

The error of the hydraulic model in predicting stage is within 0.4 m for discharges less than 1,300 m^3/s. Between 1,300-2,500 m^3/s, the model accuracy is about 1.0 m, and for discharges between 2,500-5,900 m^3/s, the model accuracy is on the order of 1.5 m.

In the absence of large floods on the flow-regulated Colorado River in Grand Canyon, the new hydraulic model and the accompanying inundation maps are a useful resource for researchers interested in water depths, shorelines, and stage-discharge curves for flows within the river corridor with 2002 topographic conditions.

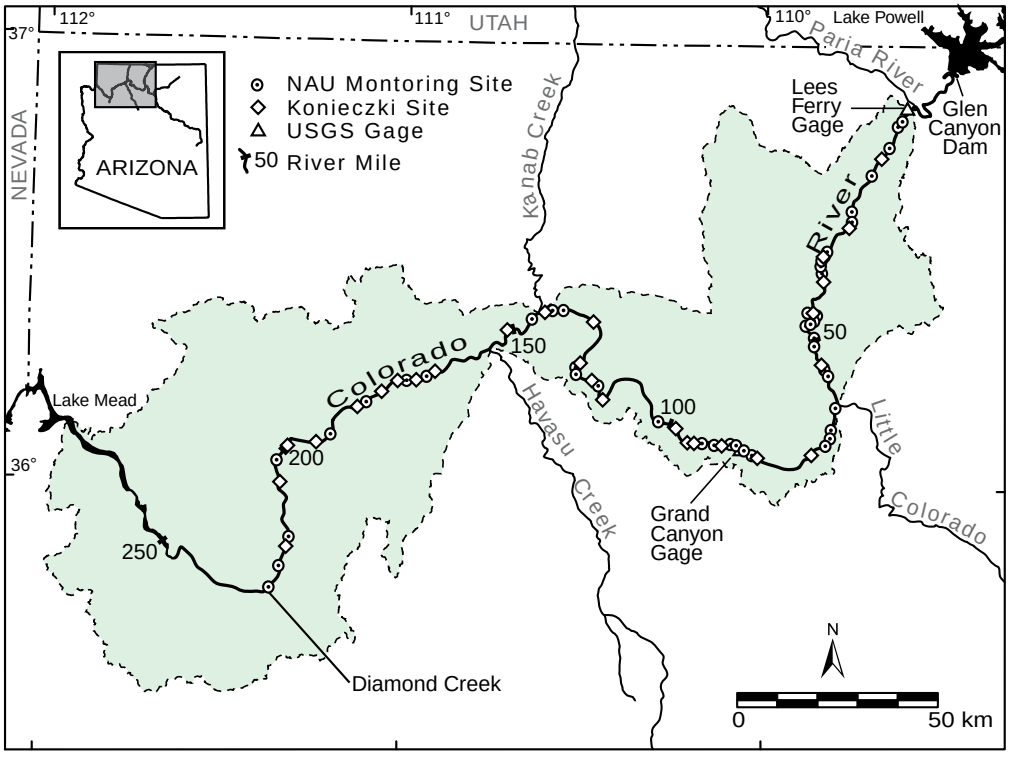

Figure 1. Map of Grand Canyon showing corridor of the Colorado River and the 45 NAU monitoring sites and 27 Konieczki sites used to evaluate the stage-discharge prediction accuracy of the hydraulic model.

Introduction

Prediction of water inundation and stage, or the height of the water surface, at a particular location is commonly needed by researchers studying various scientific questions along the Colorado River in Grand Canyon. The Grand Canyon Monitoring and Research Center's (GCMRC) Integrated Science Program (ISP) often requires stage information for many specific locations and areas within Grand Canyon to address resource issues affected by operations of Glen Canyon Dam. To estimate the river stage, particularly for floods, Grand Canyon researchers rely on predictive equations (Wiele and Torizzo, 2003), reconstructed water-surface elevations from photographs (for example, Topping and others, 2003), stage-discharge relations from temporary or established gaging stations (Gauger, 1996; Konieczki and others, 1997), or stage-discharge relations measured at specific study sites (Hazel and others, 2007). Modeled estimates of river stage are also available for 386 km of the Colorado River below Glen Canyon Dam (Randle and Pemberton, 1987), but these predictions were based on limited bathymetric data and approximate topographic data. Driftwood, flood deposits, and high-water marks determined from vegetation bands also offer clues into depth of inundation of different flows (see, for example, Draut and others, 2005). Even where stage is known, the spatial extent of inundation along the river corridor for specific discharge is unknown. Numerical models are sometimes the only way to predict water depth at particular locations in Grand Canyon for variable discharges.

Grand Canyon Geomorphology

The Colorado River in Grand Canyon has long, flat sections of quiet water separated by steep, turbulent rapids. Periodic debris flows and frequent flash flooding originating in tributaries build debris fans at tributary mouths and deposit large boulders in the river (Cooley and others, 1977; Webb and others, 1989; Melis and others, 1994; Webb, 1996). In all, 534 tributaries supply coarse-grained sediment into the Colorado River between Lees Ferry and Diamond Creek (Webb and other, 2000). The Colorado River, confined by bedrock walls, pools upstream of the accumulated debris fans before descending as rapids over the fans, commonly plunging into downstream pools and forming strong recirculation eddies below the rapids usually on both sides of the river. When viewed in profile, the water surface is stepped, termed by Leopold (1969) as a pool-and-rapid morphology. Viewed in plan, the distinct pattern of debris fans, rapids, pools, and recirculation eddies is readily apparent at most tributaries; Schmidt and Rubin (1995) called this morphology the fan-eddy complex and documented its influence on the overall geomorphic framework in Grand Canyon.

This longitudinal configuration of pools and rapids results from the dynamic interplay between the addition of coarse-grained alluvium from tributaries and the subsequent removal, or reworking, of that material by main-stem Colorado River floods (Kieffer, 1985; Webb and others, 1999). On average, about five debris flows occur each year in Grand Canyon (Griffiths and others, 2004) aggrading the river and causing the river profile to rise. Floods, in turn, act to erode this material and lower the water-surface profile. The total change in the water-surface profile near rapids can be more than a meter, occurring in a single storm or flood event (Magirl and others, 2005).

The STARS Model

Randle and Pemberton's (1987) STARS model was developed to predict sand transport down the river during typical dam releases. With closure of Glen Canyon Dam in 1963, the mean annual sediment supply at Lees Ferry of 57±3 million metric tons (Topping and others, 2000) was mostly impounded behind the dam, and the retention of sand within the river corridor to preserve camping beaches and benefit native aquatic ecology became a salient management goal (U.S. Department of Interior, 1995).

Written in Fortran and intended to be run on large mainframe computers, the STARS model was an important technical achievement at the time. The model was the first comprehensive hydraulic model built for the sizeable reach of the Colorado River between Lees Ferry and Diamond Creek (fig. 1). The STARS model was also applied to the Colorado River between Glen Canyon Dam and Lees Ferry using cross sections measured in 1990. The model used a constant Manning's n value of 0.035 for all cross sections, though roughness coefficient is less important for rapid-influenced, bedrock-controlled rivers than alluvial rivers owing to the dominant hydraulic control exerted by the rapids (O'Connor and Webb, 1988; Webb and Jarrett, 2002). Randle and Pemberton (1987) forced their model to a subcritical regime (that is, allowing conditions up to but not exceeding critical flow) assuming that while the river may be critical at each rapid, no reach of the river has supercritical flow for any significant distance. This assumption proved appropriate as the model results qualitatively captured the behavior of the river.

There were, however, understandable limitations to the model. STARS used 708 cross sections for 362 km of river, of which only 199 cross sections represented actual topography and bathymetry from Grand Canyon, all measured in pools or low-velocity reaches of the river. The other 509 cross sections, located at major rapids, were "interpolated," or constructed using aerial photography. Channel width and side slopes were estimated assuming a trapezoidal cross section. Bathymetry at each interpolated cross section was synthesized by adjusting the channel bottom up or down until the predicted water-surface profile closely matched a known water-surface profile measured along the river. This unique approach of creating synthetic bathymetry when real bathymetry is otherwise

unavailable is a powerful tool enabling the construction of hydraulic models in bedrock-controlled rivers; to the best of our knowledge, Randle and Pemberton (1987) and the Bureau of Reclamation (2001) are the only previous researchers to apply this approach. In 1987, the only available water-surface-profile data had been measured in 1923 (USGS, 1924). Because the water-surface profile in Grand Canyon is known to have changed significantly during the 20th century (Magirl and others, 2005), the STARS model better represented the state of the river in 1923, rather than the current, regulated river. Furthermore, due to the motivation to model sediment flux during smaller, dam-release flows and the lack of available topographic data, the height of each cross section in the STARS model extended above the river only far enough to accommodate a discharge up to 2,500 m^3/s. Despite these limitations, many researchers still use the predicted water-surface profiles from the STARS model to estimate stage (Bureau of Reclamation, 1996; Walters and others, 2000).

Other Grand Canyon Hydraulic Models

Bennett (1993) built on the work of Randle and Pemberton (1987), constructing hydraulic models at a reach from river miles 59.3-87.6 (Grand Canyon reach) and another short reach between river miles 164.0-166.6 (National Canyon reach) to model the movement of sands and gravels. Bennett incorporated Randle and Pemberton cross sections into his model, then added 43% more cross sections to the Grand Canyon reach and 89% more cross sections to the National Canyon reach to improve resolution. O'Connor and others (1994) constructed a small hydraulic model for a 1.2 km reach of the river near river mile 2.0 to estimate peak discharge of the paleofloods which left slackwater deposits at Axehandle Alcove.

An unsteady, one-dimensional routing model was developed for Grand Canyon. This model solved the St. Venant equations using reach-averaged normalized cross sections and predicted the routing of daily dam-released discharge waves down the river corridor (Wiele and Smith, 1996; Wiele and Griffin, 1997). This model was latter enhanced to simulate the downstream transport of fine-grained sediment in the reach from Lees Ferry to Phantom Ranch at river mile 87 (Wiele and others, 2007). Though this unsteady model is useful for predicting the propagation of a discharge wave downstream, it cannot directly predict stage or water inundation at a particular site.

Two-dimensional models have also been built for short reaches of the Colorado River in Grand Canyon. One such set of models was built for four sections of the Colorado River below the confluence with the Little Colorado River using a finite-volume approach (Wiele and others, 1996; Wiele, 1997). These Wiele models not only predicted stage and flow velocity, but also predicted the spatial aggradation or erosion of sand from the riverbed during flood conditions. Another two-dimensional model was built to simulate flow near Mohawk Canyon (river mile 172) in Grand Canyon in order to predict water surface and flow velocity (Miller and Cluer, 1998). Due to the computational complexity of running these two-dimensional models, however, only short reaches can be simulated at a time and a simulation of all of Grand Canyon would be impractical.

Purpose and Scope

With widely-available, GUI-based hydraulic software packages and an extensive, recently-collected Grand Canyon topographic data set (including LIDAR data from 2000 and photogrammetric DEMs from 2002), it became appropriate in the early 2000s to develop a new hydraulic model analogous to the STARS model, excluding sediment transport. This new model, incorporated into the HEC-RAS modeling system, uses one-dimensional, standard-step modeling to predict water-surface elevations along the main channel of the Colorado River between Lees Ferry (river mile -0.001) and the gaging station above Diamond Creek (river mile 225.228). In addition to developing an updated hydraulic model for Grand Canyon, we also developed GIS-based techniques to visualize and analyze the extent of water inundation at different discharges for any site in Grand Canyon.

The purpose of this report is to document the creation and use of the one-dimensional hydraulic model and the accompanying graphics package depicting virtual shorelines in Grand Canyon. We built the hydraulic model to simulate steady-flow discharges on the Colorado River up to 5,900 m^3/s. Estimates of the accuracy of the model are given.

Acknowledgements

Development of the updated STARS model was funded by the Grand Canyon Monitoring and Research Center of the U.S. Geological Survey, Flagstaff, Arizona. Tim Randle supplied bathymetric data and provided suggestions and insight for the construction of the model. Joe Hazel provided the latest stage-discharge data from Grand Canyon monitoring sites. Steve Young took the photograph of Boulder Narrows at low flow. David Topping provided stage-discharge data from high flows at Lees Ferry and Grand Canyon and detailed driftwood data at multiple Grand Canyon sites. Tim Randle, David Schoellhamer, David Topping, and Mike Nolan reviewed the manuscript, with David Topping providing particularly insightful comments to evaluate the validity of the synthetic bathymetry approach and to improve the overall report. Finally, Helen Fairley was instrumental in motivating and supporting the final release of this report.

Study Area, Place Names, and Units

In this report, we use metric units for all measures except river mile, which is used to describe the location along the river centerline in Grand Canyon. Though a number of river-mile conventions are available, we used the standard established by GCMRC (2002). Use of river mile has considerable historical precedent and provides a reproducible method of describing sites with respect to the Colorado River. The left and right sides of the Colorado River are determined as one faces downstream. Similarly, consistent with common practice, cross sections are displayed and described as if looking downstream.

We typically refer to "Grand Canyon" in broad reference to the Colorado River watershed between Lees Ferry and the Grand Wash Cliffs, including Marble and Grand Canyon proper. "Marble Canyon" is the canyon reach of the Colorado River between Lees Ferry and the confluence with the Little Colorado River (river miles 0 to 61.5; fig. 1). "Glen Canyon" is the reach of the Colorado River upstream from Lees Ferry, most of which has been dammed by Glen Canyon Dam (river mile -15.4). The sub reach, "Upper Granite Gorge" is the section of river between river mile 77.5 and river mile 117.8, characterized by steep, narrow walls of Precambrian bedrock (Schmidt and Graf, 1990). The sub reach, "Furnace Flats" is the section of river between river mile 61.6 and river mile 77.4 which is relatively wide, both in the channel and the overbanks (Schmidt and Graf, 1990).

Water-Surface Profile Analysis with the Standard Step Method

One-dimensional hydraulic modeling is a common technique to predict the depth of flow in natural and man-made channels. In building a model, flow is assumed to be steady and one-dimensional, gradually varied, and cross sections are constructed orthogonally to the flowing water to best represent the geometry of the river channel (Hoggan, 1997). The water surface spanning a cross section is assumed to be level, and the slope of the channel is assumed to be small. Cross sections are commonly generated using field surveys, digital elevation models (DEMs), or topographic maps, and in addition to including geometry (both above and below the existing water line), an estimate of the hydraulic roughness at the cross section is required. A full list of assumptions and techniques for one-dimensional modeling is available in Chow (1959), Davidian (1984), and Hoggan (1997).

The standard-step method is commonly used to estimate water-surface profiles in natural channels (Chow, 1959; Henderson, 1966). The method computes changes in water-surface elevation between adjacent cross sections by solving the energy equation written in the following form (fig. 2):

$$Y_i + Z_i + \frac{\alpha_i V_i^2}{2g} = Y_{i+1} + Z_{i+1} + \frac{\alpha_{i+1} V_{i+1}^2}{2g} + h_e, \quad (1)$$

where Y is the depth of the water at a given cross section, i is the index for the given cross section, i+1 is the index of the next upstream cross section (when assuming subcritical flow conditions), Z is the elevation of the main channel inverts, α is the velocity weighting coefficient, V is the average velocity at a cross section, g is the gravitational acceleration, and h_e is the energy head loss between the two cross sections. To solve equation (1), the continuity equation at each cross section is needed to calculate average velocity:

$$V = \frac{Q}{A_i}, \quad (2)$$

where Q is the discharge in the river and A is the cross sectional area of the flowing water. If the water surface is known at the downstream cross section (fig. 2), then combining equation (2) with equation (1) leaves two unknown variables, the water surface at the upper cross section and the energy loss between the cross sections. To reduce the number of unknowns downs to one, information of the energy losses is needed. Energy loss in open channels has two components,

$$h_e = h_f + h_o, \quad (3)$$

the energy loss due to boundary roughness or friction, h_f, and other (expansion and contraction) energy losses, h_o. The energy loss due to boundary roughness is approximated by,

$$h_f = \bar{S}_f L, \quad (4)$$

where $\bar{S}_f$ is the representative mean friction slope and L is the reach length between the cross sections. The friction slope, and subsequently the energy loss due to boundary roughness, is calculated using Manning's equation, an estimate of Manning's roughness coefficient (n), as well as values of conveyance calculated for different regions of the channel. The conveyance calculations are also used to estimate the velocity weighting coefficient used in equation (1). Details of the Manning's and conveyance equations and their application to the standard step method are not needed for the discussion in this report, but they can be found in Chow (1959) and Hoggan (1997). The other energy losses, h_o, appearing in equation (3) are due to expansion and contraction losses arising from eddies in the flow,

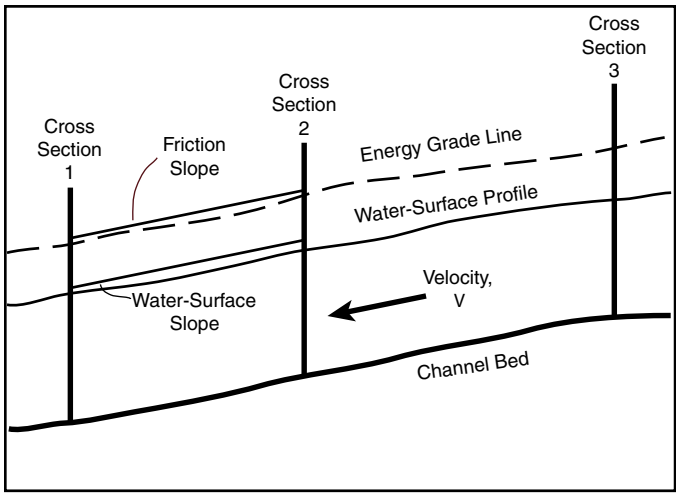

Figure 2. Schematic diagram of a longitudinal profile defining terms used in one-dimensional hydraulics.

$$h_o = C\left|\frac{\alpha_{i+1}V_{i+1}^2}{2g} - \frac{\alpha_i V_i^2}{2g}\right|, \quad (5)$$

where C is either the expansion coefficient (if the downstream velocity is less than the upstream velocity) or the contraction coefficient (if the downstream velocity is greater than the upstream velocity).

Equations (3-5) are used to solve the energy equation, but due to irregularities in natural channels, the upstream water surface cannot be explicitly solved, and an iterative set of steps is needed to determine the upstream water-surface elevation. First the water surface at the upstream cross section is assumed, and the velocity head and total conveyance at the upstream cross section is computed. With these computed values of velocity head and conveyance, the total energy loss, h_e, is computed with equation (3). The upstream water-surface elevation can then be calculated using the energy equation (1), and this water-surface elevation is compared to the water-surface elevation computed with the original assumption. If the difference between these two values is less than the accepted tolerance, the iteration is complete. If the difference between the two water-surface values is greater than the allowable tolerance, the steps above are repeated using the energy-equation computed water surface as the new assumed estimate. This iterative method is the standard-step method and is discussed in detail by Chow (1959) and Hoggan (1997).

Standard-step analysis is usually performed using a numerical model, and common computer programs for step analysis include HEC-2 (Feldman, 1981), WSPRO (Shearman and others, 1986), and HEC-RAS (Brunner, 2002). The differences among these programs are mainly the user interface and specific routines to handle flow around floodplain structures.

Hydraulic Model Construction

The new Grand Canyon hydraulic model was constructed in HEC-RAS version 3.1, a free software application developed by the US Army Corps of Engineers, Hydrologic Engineering Center (Brunner, 2002). With an integrated graphical user interface, wide acceptance, and availability of the application, HEC-RAS proved to be an appropriate development platform. The model is one dimensional and uses the standard-step approach to predict the water-surface elevation, or stage, at specific cross sections. After development of the Grand Canyon hydraulic model, the Hydrologic Engineering Center released HEC-RAS version 4.0 beta; the Grand Canyon hydraulic model is compatible with this newer HEC-RAS version.

Model Parameters

The model was run under subcritical flow conditions. Supercritical flow is not sustainable for significant distances in most natural channels (Jarrett, 1984; Trieste, 1992). For rivers flowing over an alluvial substrate in a natural channel, many postulate that supercritical flow occurs rarely, if ever (Jarrett, 1984; Grant, 1997). For this reason, it is common for researchers to run hydraulic models under subcritical conditions (Randle and Pemberton, 1987; O'Connor and Webb, 1988; Webb and Jarrett, 2002), where flow is allowed to approach, but not exceed critical depth. In Grand Canyon, where debris fans constrict the flow, HEC-RAS tends to predict critical flow at most significant constrictions, particularly for lower discharges.

The downstream cross section of the model was placed at the site of the USGS gaging station at Diamond Creek (Colorado River above Diamond Creek near Peach Springs, Arizona, 09404200) located at river mile 225.228. The downstream boundary condition was selected to be the rating curve from the gaging station. This Diamond Creek rating curve, however, is only valid for discharges up to 1,400 m^3/s. In order to model larger discharges, the shape of the adjusted rating curve from the USGS gaging station at Grand Canyon (Colorado River near Grand Canyon, Arizona, 09402500) was superimposed on the upper end of the Diamond Creek rating curve for discharges between 1,400 m^3/s to 5,900 m^3/s. The geomorphology of the river corridor near the Diamond Creek and Grand Canyon gages is similar—narrow canyon walls of Precambrian granite and gneiss—and lacking high discharge flow data measured directly at the Diamond Creek gaging station, this substitution represented a reasonable surrogate.

The contraction coefficient was kept at the default value of 0.1 and the expansion coefficient was kept at the default value of 0.3, though larger values may be appropriate for rapids reflecting abrupt transitions to better estimate the energy losses associated with recirculation eddies (Hoggan, 1997). Future versions of the model could benefit from analysis and application of more appropriate loss coefficients.

Similarly, in modeling rapids with large recirculation eddies either upstream or downstream of the rapid, the use of ineffective flow areas may improve model results. HEC-RAS allows these ineffective flow areas to be built into cross sections within models to restrict the total area in a cross section available for flow conveyance. By inserting ineffective flow areas into cross sections dominated by eddies, future versions of the model may better predict stage, particularly in sections immediately downstream of rapids.

Topographic Data and Water-Surface Profile

Topographic data used to construct the subaerial sections of the model came primarily from a data set of digital imagery and automated photogrammetry provided to GCMRC by ISTAR America, Inc. ISTAR America collected and processed images captured during a series of May 2002 Grand Canyon overflights. In addition to digital imagery, a one-meter digital elevation model (DEM) built with photogrammetry (NGVD88) was assembled for the entire river corridor. The ISTAR DEM has an absolute vertical accuracy estimated by GCMRC to be better than 0.3 m (Steve Mietz, GCMRC, written communication, 2003). ISTAR aerial photography was also used to facilitate cross-section selection.

The water-surface profile used to calibrate the model was modified from a water-surface profile constructed by Magirl and others (2005); Magirl and others used LIDAR overflight data collected in 2000 to construct their original profile. Because the hydraulic model was built from topographic data from the ISTAR America DEM, this 2000 water-surface profile was mapped onto the ISTAR America DEM and points were adjusted vertically such that the spatial coverage of the water surface closely matched the extent of the river shoreline shown in the DEM and matching imagery. Typical adjustments were less than 0.5 m. The discharge for the water surface reported by Magirl and others (2005) was 227 m^3/s, as was the discharge during the 2002 overflights used to build the DEM. This adjustment process produced a water-surface profile matching the morphology of the DEM and represents the state of the river in 2002. This 2002 water-surface profile, used for model calibration, is available in Magirl (2006).

While no independent estimate of the accuracy of the water-surface profile is available, it is possible that either the original LIDAR profile or the process of mapping this profile onto the DEM differs from the actual water-surface profile in the river. If there is a significant difference between the water-surface profile used to calibrate the model and the water-surface profile in the actual river corridor, errors could be introduced during the calibration process. This possibility will be discussed in the Synthetic Bathymetry section below.

Cross Section Locations

The locations of cross sections were chosen by following, when possible, the techniques recommended in the hydraulic literature (Benson and Dalrymple, 1967; Davidian, 1984). Ideally, cross sections would be chosen away from eddies where the entire flow field is downstream and perpendicular to the cross section. Owing to the ubiquitous distribution of eddies along the river corridor in Grand Canyon, however, it would be impractical when selecting cross sections to avoid all eddies. Many cross sections, therefore, are positioned across recirculation eddies. At each rapid, using the approach of Randle and Pemberton (1987), a group of at least four cross sections were selected: one at the head of the rapid, a second about 15 m upstream from the head, a third about 45 m upstream from the head, and a fourth cross section at the foot of the rapid. For long rapids, additional cross sections were placed within the rapid as needed to capture the fall of the water surface moving down the rapid (fig. 3). A collection of four cross sections were also placed near tributaries that flowed into otherwise slow-moving reaches of river. These tributaries, while associated with no rapid today, were assumed to have the potential to create rapids in the future. Placement of extra cross sections near currently slow-moving tributary junctures allows adaptation to future modeling of tributary input; the model can also be quickly updated in the event of a rapid-creating debris flow. In slower sections of river away from tributaries, cross sections were spaced to best capture the progression of the river following the recommendations of Davidian (1984), and cross sections were placed at river sections that widened or constricted abruptly (expansions and constrictions). To enable a comparison of the model results with the STARS model, cross sections were also generated at the locations of the 199 non-interpolated cross sections built into the STARS model.

Generating Cross Sections

A total of 2,680 cross sections were generated and built into the Grand Canyon hydraulic model covering 362 km of river from Lees Ferry to Diamond Creek. Consistent with HEC-RAS geometric conventions, each cross section was generated as a two-dimensional list of coordinates representing the station/elevation values of points along the cross section when viewed in the downstream direction. Points within a cross section were spaced, on average, about 3 m apart. The bank station for the right and left banks (that is, those points in the cross section separating the main channel from the overbank regions) was placed where the cross section intersected the river shoreline at 227 m^3/s. We determined this location using aerial imagery. The cross sections were constructed perpendicular to the river centerline and extended away from the river shorelines, up the canyon walls, far enough to incorporate 30 m vertical elevation above the water surface on both sides of the cross section. This freeboard enabled the model

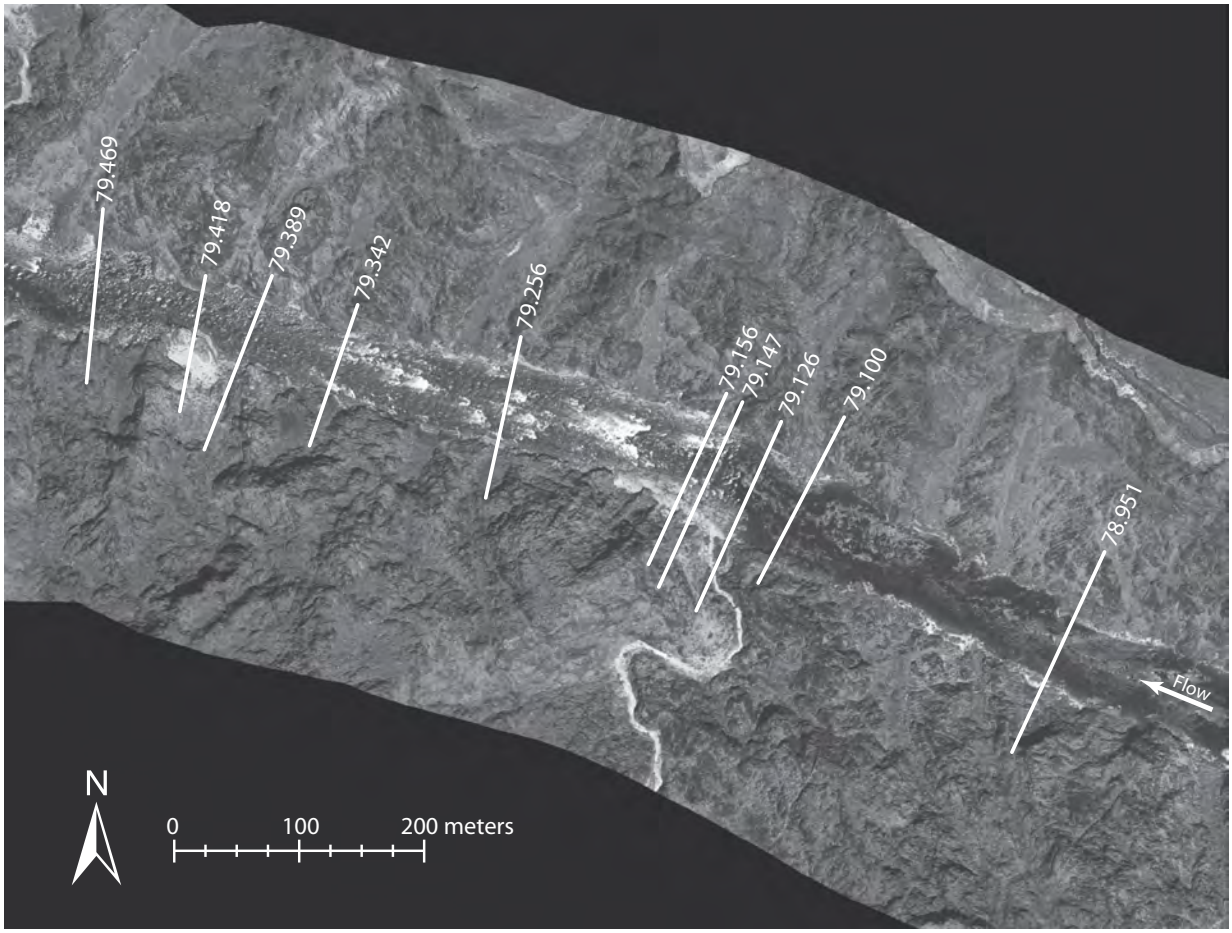

Figure 3. Cross-section locations shown for the reach of river at Sockdolager Rapid (river mile 79.1). The river-mile location appears next to each cross section. The length of each cross section represents the distance the cross section extends up the canyon walls.

to simulate discharge up to 5,900 m^3/s at every cross section. Moreover, in HEC-RAS, if the depth of the predicted water surface rises above the extent of the available cross-section geometry, the model assumes that walls rise vertically from the edge of the cross section containing the flow. Therefore, discharges higher than 5,900 m^3/s can be simulated along specific reaches where the predicted water surface overtops the existing cross sections.

In some wider sections of the river where river curvature was pronounced, distal ends of adjacent cross sections occasionally crossed over each other. While cross sections would be ideally broken at one or more points to maintain the section roughly perpendicular to the flow (Benson and Dalrymple, 1967), it was impractical to follow this labor intensive exercise when building the Grand Canyon model. Instead, we accepted that some sections may cross over each other and potentially affect the accuracy of the model. Future versions of the model may improve performance by reconstructing cross sections to avoid this interference.

In places, the DEM contains topographic surfaces that incorporate the tops of heavy stands of riparian vegetation, overestimating the true elevation of the ground. Each cross section was therefore analyzed while juxtaposed against imagery to determine areas of vegetation-influenced topography. Wherever high points in the cross section were identified with known stands of riparian vegetation, the cross section was edited to remove these higher elevation points (fig. 4). The topography under the removed vegetation was assumed to be linearly consistent with the grade away from the vegetation.

At other places within the DEM, depressions existed such that in some cross sections, DEM-obtained elevation points away from the river were below the known water-surface elevation for that cross section. These elevation artifacts were removed by manually setting the elevation at these depressed locations to the known water-surface elevation.

Within the model for a given cross section, the distances to the next downstream cross section along the centerline, along the left bank, and along the right bank are required (fig. 5). The downstream distance between cross sections along the centerline, D, is determined by location of the cross sections relative to the river centerline. To calculate downstream distance of each overbank region, the width of the river, w, the curvature of the river for the current cross section, θ_1, and the curvature of the river for the next downstream cross section, θ_2, are required. The curvature is the angle between the downstream flow vectors of sequential locations along the river; counter clockwise is positive. Once D is determined, the overbank distances are calculated using the following equations:

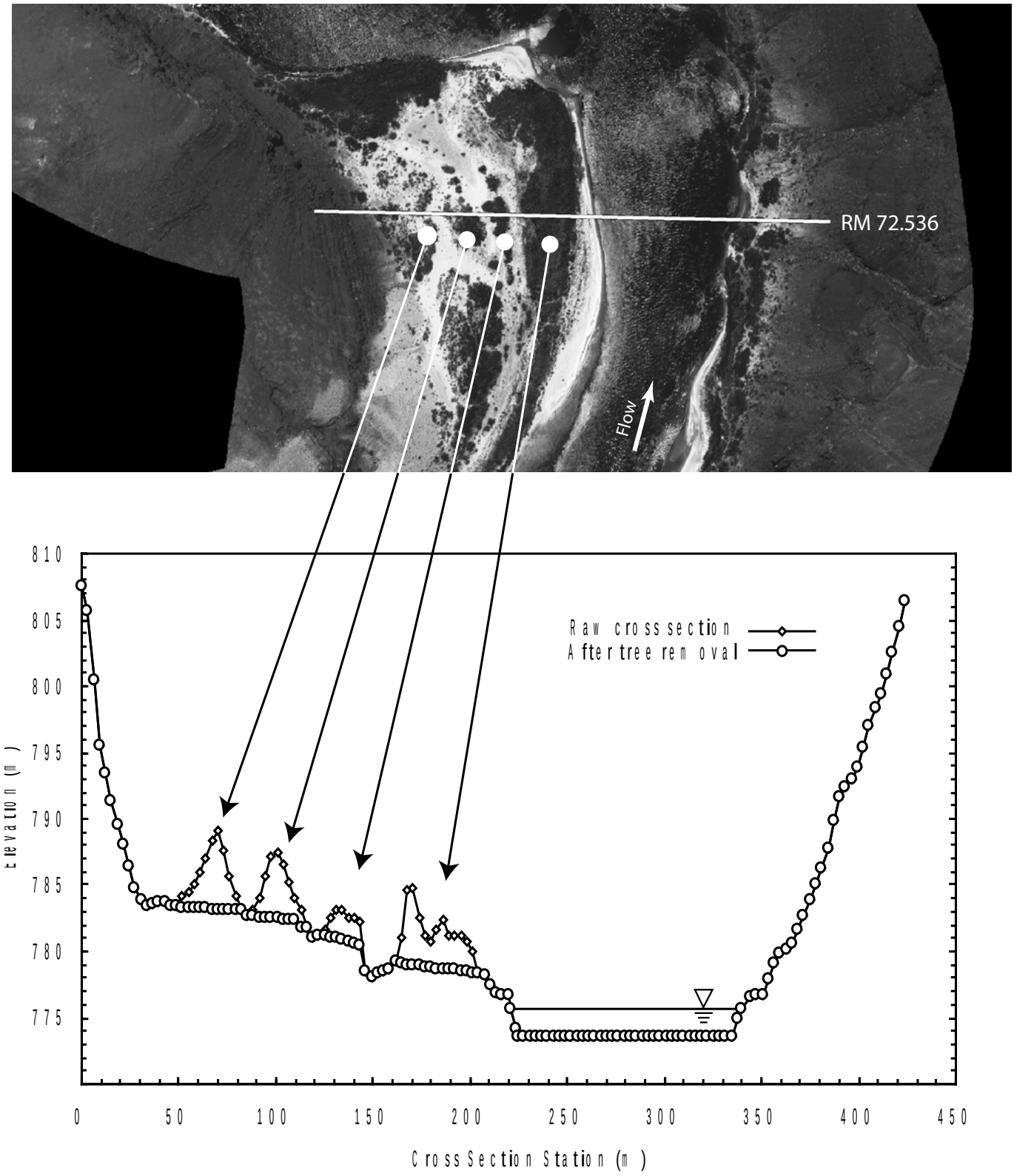

Figure 4. Cross section located at river mile 72.536 showing effect of trees on DEM topography. The top image is an aerial photo from ISTAR imagery data set; the white line represents the location of the cross section. The bottom graph shows the cross-section data (looking downstream) before and after the tree canopy was manually removed from the cross section.

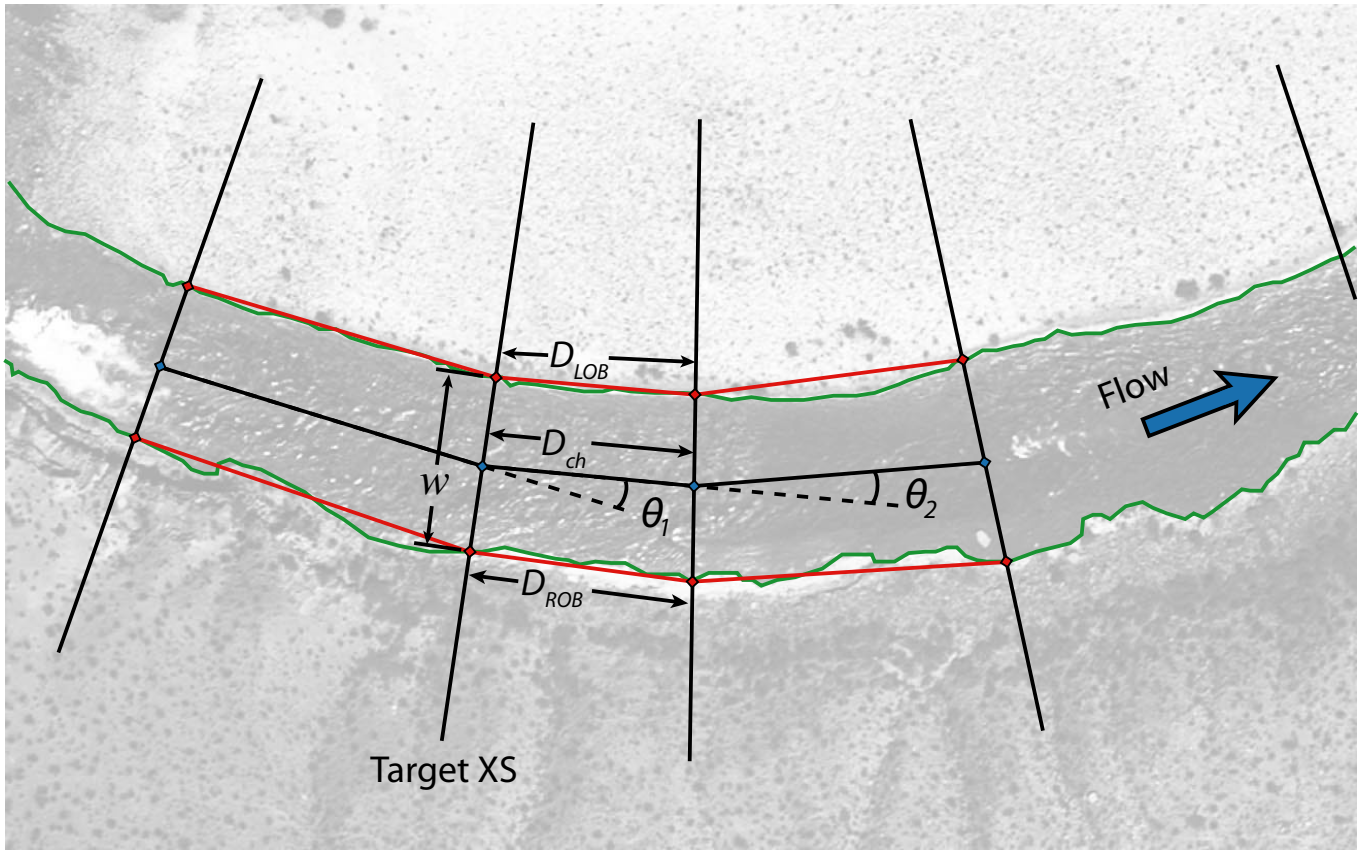

Figure 5. Sample section of river show downstream lengths for a cross section along the channel, along the left overbank, and along the right overbank.

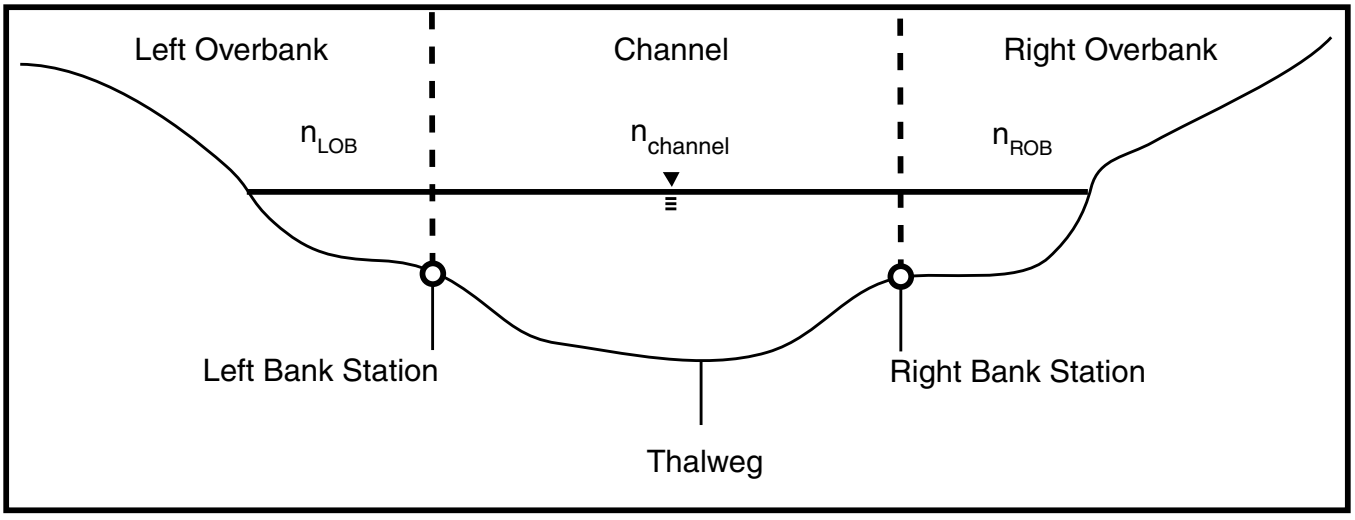

Figure 6. Schematic diagram showing definitions of terms in a channel cross section. The cross section is viewed in the downstream direction. The roughness coefficient, Manning's n, can be specified uniquely for the channel, the left overbank region, and the right overbank region.

$$D_{LOB} = D_{ch} - \frac{w}{2}(\tan\theta_1 + \tan\theta_2) \qquad (6)$$

and

$$D_{ROB} = D_{ch} + \frac{w}{2}(\tan\theta_1 + \tan\theta_2) \qquad (7)$$

Roughness Coefficient

For each cross section, HEC-RAS requires values of Manning's *n* to be specified within the channel, left overbank, and right overbank (fig. 6). However, the hydraulic model for Grand Canyon developed for this study is largely controlled by rapids located throughout the river corridor. These rapids act as hydraulic controls. Wherever flow is constricted to critical conditions in the channel, the water-surface elevation at the constriction, or the rapid, is determined by the critical depth at the constriction and not roughness coefficient. Roughness coefficient does become important, however, in determining water depth in subcritical reaches upstream from rapids. The farther upstream from a constriction, the greater the influence roughness coefficient can have on the predicted water-surface elevation. Away from cross sections with critical flow, Manning's roughness coefficient, *n*, is an all inclusive energy consumption parameter that dictates the quantity of energy head loss between cross sections through equation (1). In slow-moving alluvial rivers, energy losses are manifested through, among other things, boundary friction and sediment transport. In steep-gradient rivers, or within rapids, surface waves, extreme turbulence, and recirculation eddies consume large amounts of energy, strongly affecting the appropriate choice of Manning's *n* needed to accurately model the flow. All of these factors make the accurate selection of Manning's *n* a difficult exercise for the Colorado River in Grand Canyon.

In order to build the hydraulic model, an estimate of the roughness coefficient in the channel was needed to create the synthetic bathymetry (discussed below); the creation of the synthetic bathymetry was labor intensive, requiring over 12 months to finish. After completing the hydraulic model, a series of analyses were then done to evaluate how accurately the synthetic bathymetry represented real bathymetry. These analyses suggested how, if the model were to be reconstructed or if this technique were to be used in another river system, a more accurate model could be created. In this study, however, the labor intensive task of model construction precluded a recalibration of the model using new roughness coefficients suggested by the analyses. In other words, the model was constructed only once, and we did not have the time to rebuild the model using information from the post-construction analyses.

For the model construction and synthetic bathymetry calibration, a standard Manning's *n* roughness value of 0.035 was chosen for all channel regions during the calibration of the synthetic bathymetry (see below). The bed of the Colorado River in Grand Canyon is a mixed substrate ranging from sand with various bed forms in slow reaches of the river to cobbles and boulders where flow velocity is high or where tributaries enter the river corridor (Howard and Dolan, 1981). Just as bathymetry is generally unavailable in most reaches of river, the substrate for any given cross section is generally unknown. The roughness value (n=0.035) chosen for the channel represented a best guess synthesis of all the roughness elements of the Colorado River in Grand Canyon and is consistent with the recommendations of Chow (1959). This is also the same value of roughness used by Randle and Pemberton (1987) in calibrating the synthetic bathymetry of the STARS model.

While the roughness in overbank regions is variable, a uniform Manning's *n* value of 0.035 was also initially applied to all overbank regions. The overbank region of some cross sections spans exposed bedrock or talus slopes with large particles and little vegetation. Other cross sections have dense vegetation. Still other cross sections have vegetation close to the shoreline with open, low-roughness sections away from the shore. This initially chosen Manning's *n* value of 0.035 in the overbank area may not represent the actual value of roughness, but specific information for each of the 2,680 cross sections was not available. Thus, lacking better information to justify something different, the same Manning's *n* value (n=0.035) of the channel was applied to the overbank regions. After completing the hydraulic model, error analysis of the results indicated that adjusted roughness values improved model accuracy for discharges below 1,400 m^3/s (see Results section). A future potential model improvement would be to more accurately estimate the roughness coefficients of overbank regions for each cross section.

While hydraulic roughness is held constant with increasing discharge in the Grand Canyon hydraulic model, it is recognized that hydraulic roughness varies with flow conditions (Rouse, 1965). In steep-gradient rivers, there is evidence that hydraulic roughness decreases with increasing water depth as the size of the roughness elements on the riverbed become smaller relative to the depth of water (Jarrett, 1984). Indeed, many roughness equations predict hydraulic roughness varying inversely with water depth (Limerinos, 1970; Jarrett, 1984; Bathurst, 2002; Yen, 2002). In contrast, Kidson and others (2006) showed roughness increasing as rising stage exits the channel and enters riparian vegetation on the floodplain of the Mae Chaem River of Northern Thailand. To examine the possibility of variable roughness values impacting the hydraulic model for Grand Canyon, particularly under flood conditions, a sensitivity analysis of the final model (that is, after building the synthetic bathymetry) with different Manning's *n* values was performed. The model was run at discharges up to 1,274 m^3/s with roughness coefficients ranging from 0.025 to 0.045. The model's predicted stage-discharge behavior was then compared to the known stage-discharge curves at different sites along the river.

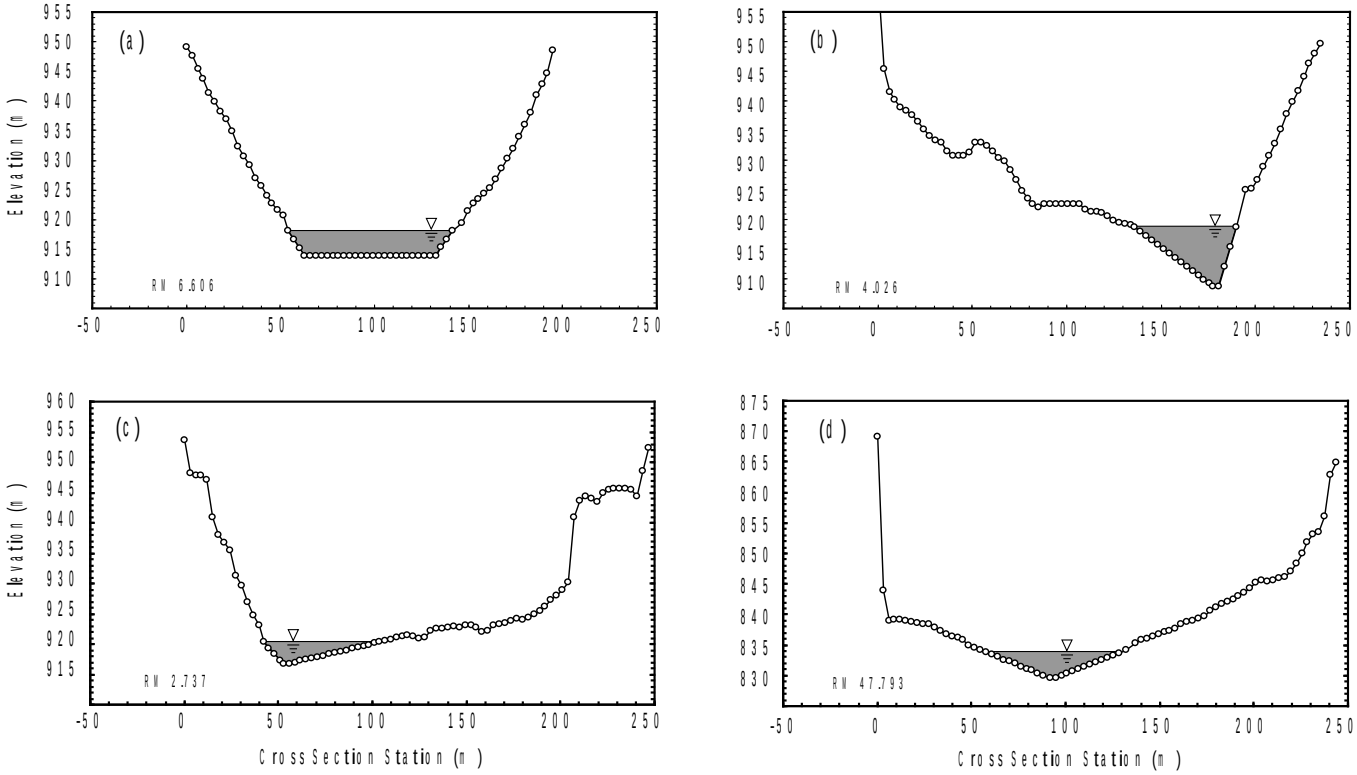

Figure 7. Example cross sections showing shape of synthetic bathymetry in (a) an open section of the river, (b) a section of river with tributary entering from river left, (c) a section of river with tributary entering from right, and (d) a section of river with tributaries entering both sides.

Synthetic Bathymetry

The cross sections built from the DEM contain only subaerial topography away from the river and no bathymetric data below the water surface. Synthetic bathymetry, therefore, was created for each cross section, mimicking the approach of Randle and Pemberton (1987). The water depth for each cross section was initially set to a value based on a bathymetric trace collected by Wilson (1986). This initial bathymetry was somewhat arbitrary and ultimately irrelevant as the bathymetric depths were later reset by the calibration process. The shape of the bathymetry at each cross section was assumed to be one of four styles based on the proximity of the cross section to tributaries (fig. 7).

For cross sections adjacent to a tributary, a triangular shape was used to best represent the subaqueous wedge of coarse-grained alluvium debouched from the tributary. For example, if the cross section was adjacent to a tributary that entered from river left, a triangular shape was chosen with the thalweg located four-fifths of the total channel width away from the left bank (fig. 7b). Similarly, for cross sections near tributaries that entered from river right, a triangular shape was chosen with the thalweg located four-fifths of the total channel width from the right bank (fig. 7c). For cross sections with tributaries entering from both sides, a triangular shape was chosen with the thalweg placed in the channel center (fig. 7d). For cross sections away from any tributary, the bathymetry was assumed to be trapezoidal with 1:1 side slopes (fig. 7a). Similarly, for the few cross sections that had an island and two separate flow channels, the bathymetry for each channel was assumed trapezoidal with 1:1 side slopes. These cross-section shapes are consistent with the trends of channel shape in Grand Canyon reported by Flynn and Hornewer (2003).

Occasionally, cross sections showed small exposed boulders in the middle of the river. These particles were, for the most part, removed from the cross section. An exception to this rule was the large boulder at river mile 18.746, several meters wide in the middle of the channel. This large boulder was retained in the model as an island.

Synthetic Bathymetry Calibration

The goal, or intent, of the calibration process was to adjust the depths of cross sections such that the model's predicted water-surface elevation matched the known water-surface elevation to within a predetermined tolerance limit. During the model calibration, the target tolerance between the known and predicted water-surface profiles was 30 mm and the calibration discharge was 227 m^3/s. All synthetic-bathymetry calibration was done with a constant Manning's roughness coefficient of n=0.035. Owing to the subcritical nature of the hydraulic model, calibration started at the farthest downstream cross section, working upstream until the entire model was calibrated. When changing bathymetry, station/elevation points within that cross section below the known water-surface elevation were adjusted vertically; the adjustment at a particu-

lar station/elevation point was made proportionately according to the relative depth of the point so that the shape of the bathymetry at that cross section remained consistent. Adjustments that would result in a water depth less than 1.52 m were not made; in other words, the minimum allowable water depth for a cross section was 1.52 m. This minimum depth was chosen arbitrarily.

The calibration process began by inspecting the difference between the predicted and known water-surface elevations at the target cross section. The synthetic bathymetry was then raised or lowered at the target cross section and its closest downstream neighbors (the downstream neighbors also needing adjustment due to the hydraulic influence from downstream control in subcritical flow). After rerunning the hydraulic model, a new predicted water-surface profile was again compared to the known profile, thus suggesting a change value for the next adjustment. By iteratively evaluating water-surface elevation difference, adjusting bathymetry, then reevaluating the difference, the predicted water-surface elevation at the target cross section eventually approached the known water surface. If the difference between the predicted and known water-surface elevation was less than the accepted tolerance, the next upstream cross section became the new calibration target. If it became apparent the hydraulic conditions at the target cross section would not permit a calibration within the tolerance limit, an attempt was made to minimize the difference then the process was moved on to the next upstream cross section.

For the final calibrated model (a total of 2,680 cross sections), 88% fell within the target error tolerance of 30 mm. Most of the cross sections with error greater than 30 mm were confined to rapids or other high-gradient sections of the river. These high-gradient sections were problematic for the calibration process. An underlying assumption of the model is that flow in the river is one dimensional, but flow in a fan-eddy complex is three-dimensional with large vertical velocities in the rapid, and two-dimensional eddy structures both upstream and downstream from the rapid. Therefore, the target tolerance in and immediately downstream from rapids was, at times, discarded in favor of accuracy in the pools upstream of the rapids. In fact, the standard approach of the calibration process near rapids was to first correct the predicted water surface in the pool at the head of the rapid, then attempt to match the water-surface profile in the core of the rapid as closely as possible. Examining the model calibration only in the pools (that is, cross sections where the water-surface slope from the next upstream cross section is less that 0.001), 98.0% of the calibrated predictions were within the 30 mm tolerance and 99.8% were within 60 mm of the known water-surface elevation.

Expansion and contraction near rapids, combined with the model's attempt to preserve conservation of mass, resulted in troughs (that is, lowered water-surface elevations at the constrictions) in the longitudinal water-surface profile. Within flumes experiencing controlled and one-dimensional flow conditions, these troughs are readily observed at constrictions (Chow, 1959), but troughs have not been observed in the natural channel and three-dimensional flow conditions of the Colorado River in Grand Canyon. Energy consumption by turbulence, breaking waves, and recirculation eddies in rapids create conditions where troughs do not occur. The one-dimensional numerical model, not able to replicate the complex mechanics of the rapids, tends to predict the presence of troughs, particularly for higher discharges. Users of the model need to be aware of these water-surface elevation troughs for two reasons: (1) one-dimensional hydraulics do not apply to rapids—the model should not be used to make precise predictions about the water-surface elevation within rapids—and (2) the user should post-process all water-surface profiles taken directly from HEC-RAS by backfilling all water-surface trough from downstream to upstream. More importantly, users need to understand that the model is best at predicting the water-surface elevation in the pools above rapids, not directly in rapids nor in the eddy-dominated flow of the expansion below rapids.

Evaluating Synthetic Bathymetry

When typically building standard-step hydraulic models, the topography of the river channel, either known or measured, is first built into the model geometry. Next, a reasonable approximation of the roughness coefficient is made to enable the model to make hydraulic predictions. Finally, if available, high-water marks of known discharge are compared to the model results, thus suggesting how roughness coefficient may be adjusted to improve the model performance.

In the case of modeling the Colorado River in Grand Canyon, where bathymetric data are largely unavailable, we were forced first to assume a best guess roughness coefficient, then create synthetic bathymetry in order to build the model. As far as we know, this approach was used just twice previously, by Randle and Pemberton (1987) and by the Bureau of Reclamation (2001), but if this approach of using synthetic bathymetry can produced useful results, this technique offers a valuable, alternative way to construct hydraulic models without knowledge of the bathymetry of the river channel. The technique could be particularly useful in modeling bedrock-controlled rivers where bathymetry is difficult or impossible to measure. Because the technique of using synthetic bathymetry is both unorthodox and potentially valuable, additional analysis of the quality of the final synthetic bathymetric product was warranted.

Cross sections of the final calibrated model were compared to real bathymetric data measured by Northern Arizona University (NAU) in May 2002 through the GCMRC research program (Matt Kaplinski, Northern Arizona University, written communication, 2008). These actual bathymetric data were not available when the hydraulic model was built and therefore were not incorporated into the model; future versions of the hydraulic model could incorporate these data. In all, direct comparisons of the synthetic and actual bathymetry were made at 169 NAU cross sections located at monitoring reaches

distributed throughout the river corridor. These cross sections were measured in pools and slow water between rapids and no cross sections were measured directly in rapids. The hydraulic radius of the wetted cross section was used to compare the data sets. Hydraulic radius is given by (Chow, 1959)

$$R_h = \frac{A}{P}, \quad (8)$$

where P is the length of the wetted perimeter along the bottom of the cross section.

The accuracy of the synthetic bathymetry was also evaluated by comparing predicted water velocity from the hydraulic model with water velocity data collected in the 1990s. The mean velocity of any cross section in the hydraulic model is calculated using equation (2). Combining the mean velocity of adjacent cross sections, the predicted mean velocity of the model through any reach can be calculated. These predicted mean velocity values were then compared to velocity data collect at steady low discharge (Graf, 1995) and steady high discharge (Konieczki and others, 1997).

Finally, we conducted a sensitivity analysis on the synthetic bathymetry using variable Manning's roughness coefficients. Because the selection of roughness coefficient may be the largest source of error in generating synthetic bathymetry, the intent of the sensitivity analysis was to estimate what may have been a better choice of Manning's n for the river channel when constructing the overall synthetic bathymetry. Two short reaches of the river were chosen for the sensitivity analysis: the first reach was near Anasazi Bridge between river miles 42.669-45.453, a section of the river characterized by numerous debris fans and recirculation eddies, and the second reach was in Inner Granite Gorge between river miles 86.567-87.946, a relatively straight, narrow section of the river with relatively few recirculation eddies. Using the calibration technique described above, three different sets of synthetic bathymetry was generated in each reach using Manning's roughness values of n=0.020, 0.035, and 0.050. The synthetic bathymetry from each unique calibration was then compared to the known NAU bathymetric data described above. In addition to comparing hydraulic radius, the wetted area, A, of the cross sections was compared as well as the hydraulic depth, given as (Chow, 1959),

$$D_h = \frac{A}{T}, \quad (9)$$

where T is the top width of the water in the cross section. While the labor-intensive nature of constructing the hydraulic model precluded recalibration using roughness values suggested by the sensitivity analysis, the analysis results indicate how a future modeling effort might create more accurate synthetic bathymetry.

Estimating Model Accuracy

The accuracy of the hydraulic model's prediction is affected by prediction errors inherent in the model as well as errors built into the DEM used to construct the geometry in the hydraulic model. Because the model was calibrated to a flow of 227 m^3/s, the accuracy of the model at this discharge is presumably as good as the DEM used to build the model plus the 30 mm calibration tolerance. As discussed earlier, the DEM has an absolute vertical error estimated to be less than 0.3 m.

To estimate the accuracy of stage predicted by the final, calibrated hydraulic model, a comparison of the model's output to known stage data measured along the Colorado River in Grand Canyon is needed. To estimate error for this study, the results from the hydraulic model for discharges up to 2,500 m^3/s were compared to stage-discharge relations measured at several monitoring sites by NAU and by Konieczki and others (1997); for flows above 2,500 m^3/s, model predictions were compared to stage-discharge curves from permanent USGS gaging stations and to driftwood left at select sites along the river.

The NAU stage-discharge data were collected in the early 2000s, and the data are reported in NGDV88 ellipsoid vertical coordinates, allowing a direct comparison with the model's results. Under a long-term monitoring program, NAU routinely measures topography and stage at 47 locations in Grand Canyon, constructing stage-discharge relations for the sites at flows from 142 to 1,300 m^3/s spanning the range of flows seen in Grand Canyon over the past 20 years (Hazel and others, 2007). Of the 47 locations, 45 were within the domain of the hydraulic model and used for error analysis. Using high-water marks from the 1983 flood and driftwood left by historic floods, NAU was also able to extend the rating curves up to 2,500 m^3/s at four monitoring sites (Vaseys Paradise, river mile 32.17; Palisades, river mile 66.1; Comanche, river mile 68.3; 220R, river mile 220.065). These sites were used to calculate error from 1,400-2,500 m^3/s. For a given NAU site, the predicted water-surface elevation from the hydraulic model was calculated by linearly interpolating values from the two cross sections in the model bounding the NAU site.

The residual, or the difference between the model prediction and the known NAU stage, for a given discharge was calculated at each site. But the residual at one location did not fully represent the uncertainty of the model's predictions at other sites. To estimate the overall accuracy of the model as applied to the entire river, residuals were calculated for all NAU monitoring sites and averaged, then the standard deviation of the residuals was calculated to get an estimate of the confidence intervals of the model prediction for a given discharge. The total estimated error for the model was determined to be the standard deviation of the residuals added to the residual mean. The model error (residual mean plus the residual standard deviation) represented the total error of the model prediction to a stated confidence interval. For example, if the total error was 1.0 m, then the model would be capable

of predicting stage at any location to ±1.0 m with a confidence of 68% (that is, one standard deviation). The percent error was calculated by normalizing the total error against an estimate of relative stage. This estimate of relative stage was calculated to be the difference in height between the stage of interest and the water-surface elevation at zero discharge (0 m^3/s). The water-surface elevation at zero discharge was estimated by extrapolating the known NAU water-surface elevations at 227 m^3/s and 141 m^3/s down to 0 m^3/s.

As a secondary check of the error estimates generated using the NAU data, model predictions were also compared to stage data collected at 27 sites during the 1996 high-flow experiment (Konieczki and others, 1997). These sites were distributed widely throughout Grand Canyon (fig. 1) and measured stage at a steady flood discharge of 1,322 m^3/s and a steady post-flood discharge of 237 m^3/s. The differences in measured stage for these two discharges were then compared to the hydraulic model predictions to calculate residual mean and the standard deviation of the residuals based on the Konieczki and others (1997) data.

While other stage data were measured at temporary and permanent gaging stations throughout the river corridors during the 1980s and 1990s (see Garrett and others, 1993; Gauger, 1996; Rote and others, 1997), these data were not generally tied to discharge data. In addition, potential changes in the water-surface profile in intervening years may increase uncertainty in comparing these older stage-discharge data to the river profile in 2000-2002. Ultimately, these additional data were not of sufficient quality (nor did they offer unique information) to merit inclusion in the error analysis.

To estimate error for flows above 2,500 m^3/s, stage-discharge curves from USGS gaging stations at Lees Ferry (Colorado River at Lees Ferry, Arizona, 09380000) and Grand Canyon (Colorado River near Grand Canyon, Arizona, 09402500), as reported by Topping and others (2003), were used. To directly compare these curves, the USGS stage data were adjusted vertically to match the DEM water-surface elevation at 227 m^3/s. While data from only two gaging stations do not allow a full statistical analysis of the model's accuracy for extreme floods, these stage-discharge data allowed a rough estimate of how reasonably the model predicts stage for flows up to 5,900 m^3/s. In addition, the model output was analyzed against driftwood strand lines and driftwood piles located below Palisades Creek and at Granite Park (river mile 209) to compare model performance during large flows.

Virtual Shoreline Construction

The first step in developing virtual shorelines of water inundation was to produce a dense linear network of stage-elevation locations along the centerline of the Colorado River from Glen Canyon Dam to Lake Mead. This linear array of points was constructed by sub-dividing GCMRC's 100-meter Colorado River centerline coverage (GCMRC, 2002) into nearly 73,000 5-meter increments, or centerline points located between Lees Ferry and Diamond Creek. Water-profile data from the hydraulic model were then projected onto these centerline points by linearly interpolating values between the bounding upstream and downstream cross sections. Owing to the density of cross sections in the model, it was assumed that the water-surface elevation between cross sections was linear.

The second step was to project these water-surface data across the width of the river corridor, orthogonal to the centerline points. We constructed a two-dimensional grid of 5-meter cells extending across the width of the Canyon and coded each cell to its nearest 5-meter centerline point. The water-surface data along the centerline were then projected to the appropriate 5-meter cells, enabling the two-dimensional mapping of the shoreline at various discharges.

Virtual shorelines and inundation regions were then constructed by subtracting the two-dimensional grid representing the water surface from the DEM of the Canyon. The 5-meter stage-elevation grid was first re-sampled to 1-meter to match the spatial resolution of the DEM. Shorelines were generated by converting all negative grid cells into contiguous-area polygons. This three-step methodology was automated as an ARC Macro Language (AML) program.

Note that while known vegetation artifacts were removed from cross sections used to build the hydraulic model, vegetation stands were not removed from the base DEM used to display the virtual shorelines. As a result, polygons around stands of tree can be seen in the resulting inundation maps.

Results

First, the synthetic bathymetry was analyzed and evaluated against (where available) known hydraulic data measured in the river. Secondly, the Grand Canyon hydraulic model and the accompanying virtual shorelines were tested under a number of discharge values ranging from 142 m^3/s up to 5,900 m^3/s. For the hydraulic model runs, inundation maps were generated thus showing the location of shorelines along the river corridor. A summary of some of the important flow values modeled in the study is shown in table 1.

Analysis of Synthetic Bathymetry

Table 2 reports results of the comparison of hydraulic radius between known bathymetric data measured by NAU and the synthetic bathymetry of the hydraulic model. The NAU data were grouped into nine separate reaches, and comparisons made in each of the reaches showed that the hydraulic model consistently predicted a hydraulic radius less than reality. Overall, the mean hydraulic radius reported by NAU was 4.69 m and the mean hydraulic radius predicted by the hydraulic model for the same 169 cross sections was 3.09 m, a difference of -1.60 m. In other words, the synthetic bathymetry predicted a mean hydraulic radius 34% smaller than reality.

Table 1. Significant flows simulated in this study.

Discharge (m^3/s)	Discharge (cfs)	Significance
227	8,000	Typical flow during GCMRC remote-sensing overflights
566	20,000	Typical high flow in dam-regulated regime
1,270	45,000	Approximate size of the 1996 Controlled Flood
2,750	97,000	Approximate size of the 1983 flood, the largest post-dam flood
3,000	106,000	Approximate size of the 1958 flood
3,500	125,000	Approximate size of the 1957 flood, the most recent pre-dam flood
4,800	170,000	Estimated size of the 1921 flood[1]
5,900	210,000	Estimated size of the 1884 flood[1]

[1]As reported by Topping and others (2003)

These results indicate that the Manning's *n* used to calibrate the synthetic bathymetry (*n*=0.035) was perhaps too small. If the roughness coefficient in the real channel is larger than the value assumed when calibrating synthetic bathymetry, then more energy would need to be consumed in the model such that the predicted water-surface profile would closely match the actual water-surface profile at 227 m^3/s. Therefore, the depth in the cross sections of the final calibrated synthetic bathymetry would be smaller, resulting in smaller hydraulic radii, to compensate for the energy losses needed to predict the water surface.

The velocity data show that the predicted velocity values of the hydraulic model were 59% greater than the measured velocity data for low discharges of about 430 m^3/s (table 3). Similarly, the predicted velocity values of the model were 40% greater than actual velocity data for intermediate flows of about 1,300 m^3/s (table 3). Again, these data indicate that the cross sections in the synthetic bathymetry are shallower than the cross sections in the actual river. This result also indicates that a larger Manning's *n* would probably have led to the creation of a more accurate synthetic bathymetry.

The results of the sensitivity analysis at Anasazi Bridge (table 4) further support the conclusions drawn from comparisons of synthetic bathymetry to real bathymetry and the velocity data. As Manning's *n* increased from 0.020 to 0.050, the recalibration of the model showed that in this reach of river, the mean water area increased from 194 to 330 m^2, the hydraulic depth increased from 1.98 to 3.37 m, and the hydraulic radius increased from 1.96 to 3.27 m. In contrast, the NAU data show that the actual water area is 521 m^2, the actual hydraulic depth is 5.13 m, and the actual hydraulic radius is 4.89 m. More telling, when the results of the sensitivity analysis are extrapolated to larger roughness values, a Manning's *n* of 0.092 would be needed by the model to match the actual water area, a Manning's *n* of 0.087 would be needed to match the actual hydraulic depth, and a Manning's *n* of 0.086 would be needed to match the actual hydraulic radius. As a function of river mile, figure 8 shows the hydraulic radius for each sensitivity calibration as well as the actual hydraulic radius measured by NAU. Except for the cross sections upstream of river mile 43.4, the results of the sensitivity analysis show the synthetic bathymetry is typically smaller than the actual river. Note that some cross sections were located in rapids and the bathymetry here was not measured by NAU.

The results of the sensitivity analysis for the reach in Inner Granite Gorge are shown in table 5. In contrast to the river near Anasazi Bridge, the river in Inner Granite Gorge is steep and narrow, with few recirculation eddies. But similar to the results of the sensitivity analysis for the river near Anasazi Bridge, the sensitivity analysis in Granite Gorges shows that a Manning's *n* significantly larger than 0.050 would probably be needed to create a synthetic bathymetry that accurately simulates the hydraulic parameters of the river. For example, by extrapolating roughness values, it appears a Manning's *n* of 0.075 would be needed to match the measured water area of 377 m^2, a Manning's *n* of 0.074 would be needed to match the measured hydraulic depth of 6.48 m, and a Manning's *n* of 0.068 would be needed to match the measured hydraulic radius of 5.38 m.

The evaluation of the synthetic bathymetry using known bathymetry, velocity data, and the two sensitivity analyses suggest that if the model were going to be constructed again, a larger roughness coefficient could enable the synthetic bathymetry to more accurately match the bathymetry in the actual river. The need for a larger roughness coefficient in the model for calibrating synthetic bathymetry does not result from roughness elements in the channel requiring a larger Manning's *n*—based on the bed material and morphology, the choice of Manning's *n* of 0.035 is reasonable for the main channel. Instead, there are other sources of energy losses in the hydraulic system requiring the model to have a larger overall roughness coefficient during calibration. For example, the ubiquitous nature of recirculation eddies in the actual river may require the synthetic bathymetry to be shallower than reality in order to accommodate the observed energy losses. Also possible, inaccuracies in the water-surface profile of the river used to calibrate the synthetic bathymetry may result in a bias built into the synthetic bathymetry. If the water-surface profile used for calibration, for example, was biased in such a way that the pools were steeper than reality, the synthetic bathymetry would need to be made shallow to compensate for energy losses in the pools suggested by the steeper profile. Regardless of the reason for the inaccuracy in the synthetic bathymetry, if a higher roughness coefficient were used to

Table 2. Mean hydraulic radius in nine reaches as measured by Northern Arizona University and as predicted by the Grand Canyon hydraulic model.

River Miles	Number of cross sections	Mean hydraulic radius, measured (m)	Mean hydraulic radius, predicted (m)	Difference (m)	Percent difference
1.105-2.638	16	3.89	3.12	-0.77	-20%
21.888-23.664	23	4.76	2.60	-2.16	-45%
29.881-32.000	28	5.19	2.96	-2.23	-43%
42.669-45.453	20	4.89	3.42	-1.47	-30%
54.484-56.271	13	3.44	2.94	-0.50	-14%
63.569-66.083	20	4.75	2.99	-1.76	-37%
86.567-88.097	13	5.16	3.72	-1.44	-28%
119.319-122.397	26	4.90	3.29	-1.61	-33%
208.038-209.101	10	4.34	2.86	-1.48	-34%
Total	**169**	**4.69**	**3.09**	**-1.60**	**-34%**

Table 3. Comparison of measured and model-predicted water velocity at low flow and high flow for the Colorado River in Grand Canyon.

River Miles	Q (m^3/s)	Measured Velocity [1] (m/s)	Predicted velocity (m/s)	Difference
0.0-35.9	425	0.87	1.44	
35.9-61.1	425	0.75	1.28	
61.1-76.6	430	1.1	1.43	
76.6-117.6	433	0.97	1.83	
117.6-166.5	436	1.1	1.71	
166.6-213.5	436	1.1	1.64	
Mean		**0.98**	**1.56**	**+59%**
0.0-7.9	1276	1.51	1.91	
7.9-35.9	1276	1.69	2.59	
35.9-61.1	1276	1.49	2.15	
61.1-76.6	1327	1.9	2.40	
76.6-122.0	1327	1.93	3.07	
122.0-166.5	1327	1.89	2.89	
166.5-183.0	1327	2.11	2.51	
183.0-225.0	1327	1.83	2.61	
Mean		**1.79**	**2.52**	**+40%**

[1]As reported by Graf (1995) for low flow and Konieczki and others (1997) for high flow.

Table 4. Change in mean hydraulic parameters for a discharge of 227 m^3/s as a function of Manning's roughness coefficient for the reach near Anasazi Bridge (river miles 42.669 to 45.453). Also shown are the hydraulic parameters measured from available bathymetric data and the approximate roughness needed by the hydraulic model to match the measured data.

Manning's Roughness	Water Area (m^2)	Hydraulic Depth (m)	Hydraulic Radius (m)
0.020	194	1.98	1.96
0.035	264	2.73	2.67
0.050	330	3.37	3.27
Measured data:	**521**	**5.13**	**4.89**
Roughness needed to match measured data:	**0.092**	**0.087**	**0.086**

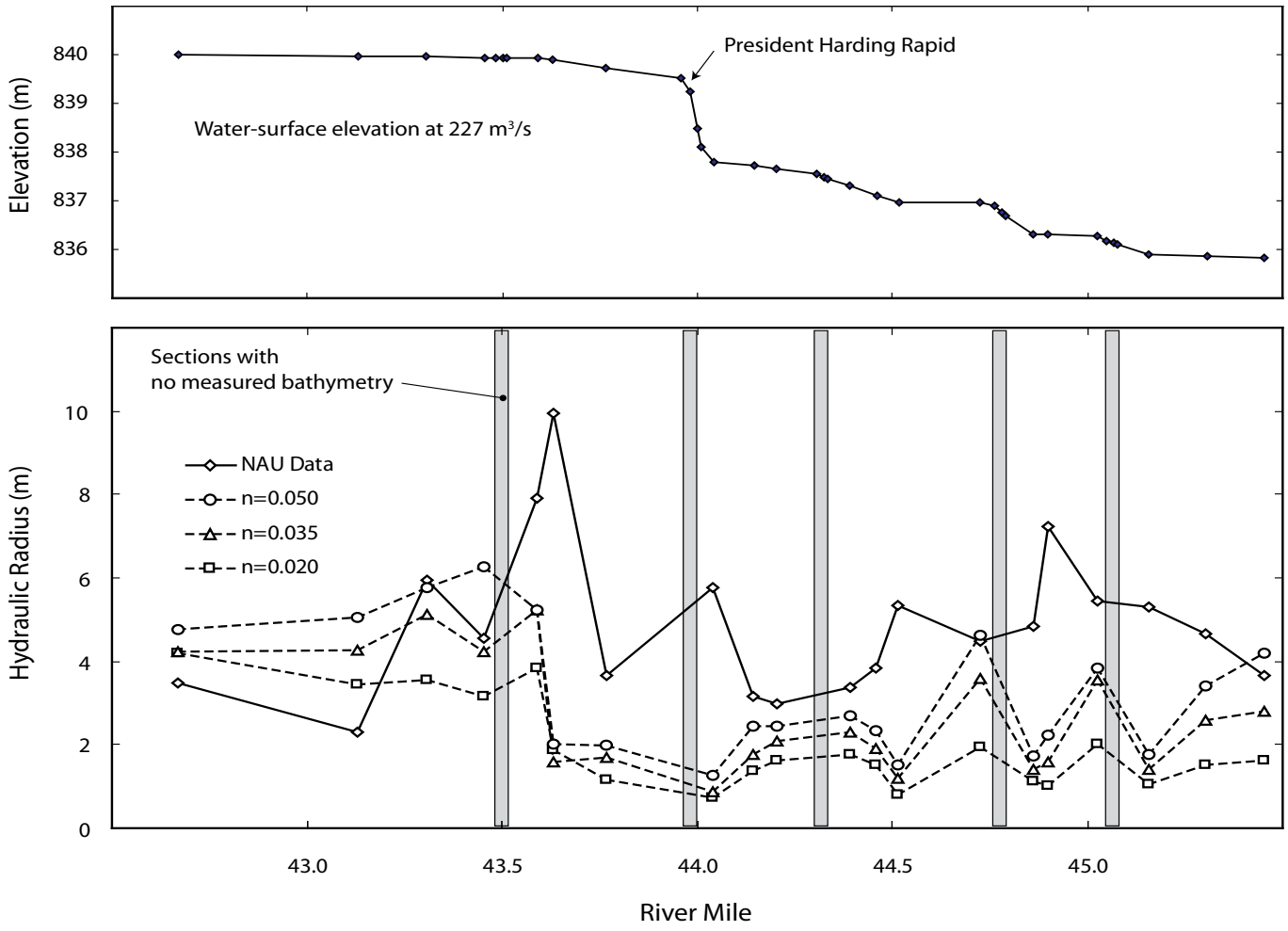

Figure 8. (Top) The water-surface profile near Anasazi Bridge showing President Harding Rapids and several downstream rapids. (Bottom) Results of the sensitivity analysis near Anasazi Bride showing the actual hydraulic radius measured by NAU and the hydraulic radius as predicted by the model calibrated for Manning's n values of 0.020, 0.035, and 0.050. The vertical gray bars shows areas where no NAU data are available.

Table 5. Change in mean hydraulic parameters for a discharge of 227 m^3/s as a function of Manning's roughness coefficient for the reach of river in Inner Granite Gorge (river miles 86.567 to 87.946). Also shown are the hydraulic parameters measured from available bathymetric data and the approximate roughness needed by the hydraulic model to match the measured data.

Manning's Roughness	Water Area (m^2)	Hydraulic Depth (m)	Hydraulic Radius (m)
0.020	169	2.97	2.84
0.035	237	4.17	3.85
0.050	282	4.93	4.44
Measured data:	**377**	**6.48**	**5.38**
Roughness needed to match measured data:	**0.075**	**0.074**	**0.068**

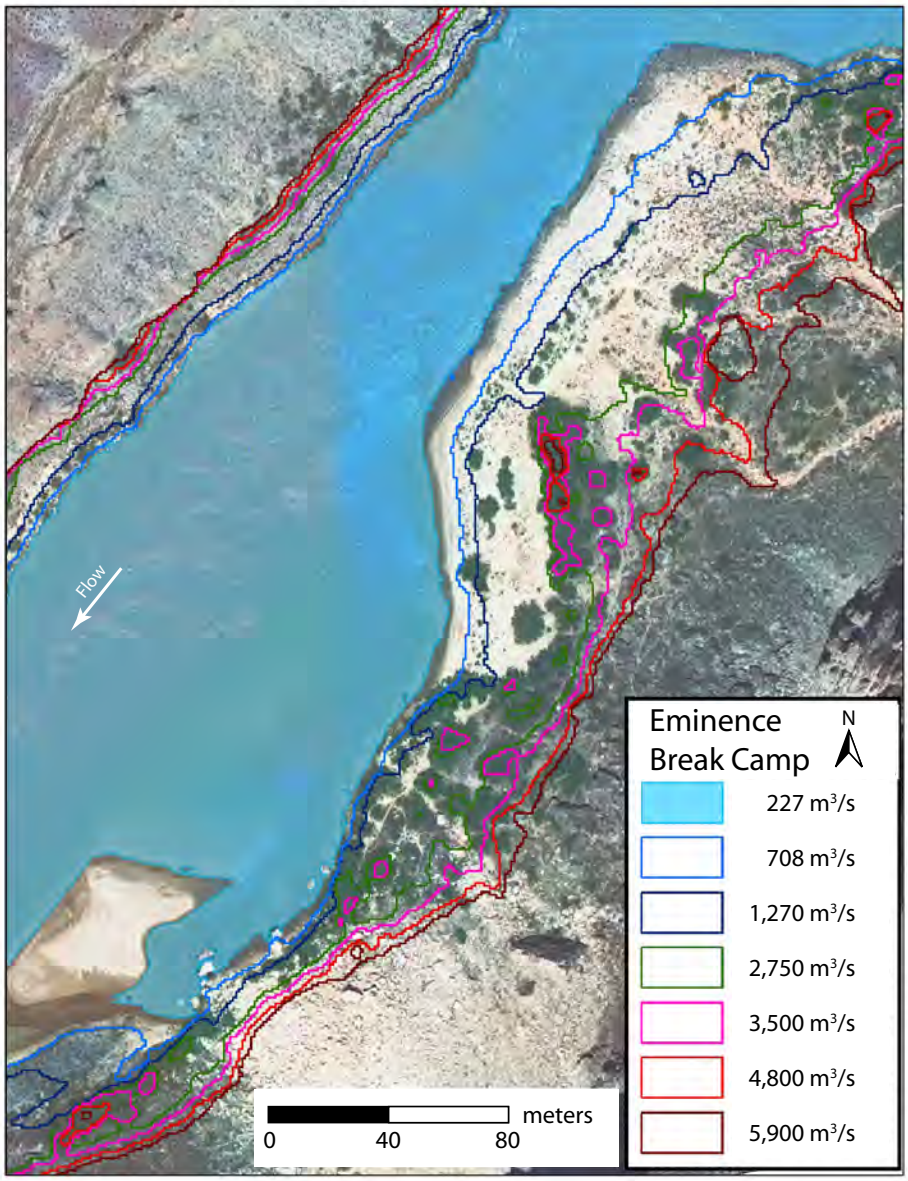

Figure 9. Virtual shorelines at Eminence Break Camp (river mile 44.5). Vegetation surface elevations can be clearly seen as island polygons.

recalibrate the synthetic bathymetry, the performance of the model for flows larger than 227 m^3/s suggests lower Manning's *n* values (on the order of 0.025 to 0.035) would be needed with rising discharge in the main channel and the overbanks. Such variable roughness values, changing spatially and with discharge, would greatly increasing the complexity of the model, and would probably be impractical for a model of this size.

Nonetheless, the reader needs to be aware that the synthetic bathymetry is 30-40% shallower than the actual river and that the predicted mean velocity in the reaches are as much as 60% faster than the velocity found in the river. Despite the inaccuracies in the synthetic bathymetry, the model can still predict stage to some level of accuracy, the quantification of which will be discussed below.

Inundation Maps

Figure 9 shows an example of the virtual shorelines generated from the hydraulic model at Eminence Break Camp near river mile 44.5. The flow in the river is from top to bottom and a relatively flat deposition bar on river left shows a large change in shoreline position with a modest rise in stage. The DEM contains a combination of bare ground and vegetated surface elevations, which are not true ground elevations but instead are artifacts of DEM construction. Virtual shoreline intersections with vegetated areas were readily apparent, as they formed island polygons and other convex patterns, visible on the map for Eminence Break Camp (fig. 9). For this site, the hydraulic model tended to under predict the water-surface elevation for flow greater than 400 m^3/s. The largest residual was -0.32 m for a discharge of 878 m^3/s, a percentage error of 10%. At a discharge of 1,274 m^3/s, the residual, is -0.25 m (fig. 10).

Comparison of the model predictions with other NAU sites gave better results. At Dino Camp, for example, the model showed good agreement with the NAU data (fig. 11). Similar to the results at Eminence Break Camp (fig. 9), the model under predicted the water surface for intermediate flows of 500-1,200 m^3/s. The largest residual was -0.16 m at 878 m^3/s, representing an error of 4%. At 1,274 m^3/s, the model under predicted the water surface by -0.08 m (5% error). The virtual shorelines at Dino Camp, therefore, represent a shoreline map that is relatively close to actual shorelines at most discharges (fig. 12).

Accuracy Estimate for flows under 1,400 m^3/s

Figure 13 shows the residual mean and standard deviation of the residuals of the hydraulic model for a range of discharges calculated from the NAU sites; table 6 lists the data used to construct the figure. Figure 13 shows that the mean of the residuals is smallest for a discharge of 283 m^3/s. At the calibration discharge of 227 m^3/s, the residual mean was 0.03 m, the standard deviation of the residuals is 0.30 m,

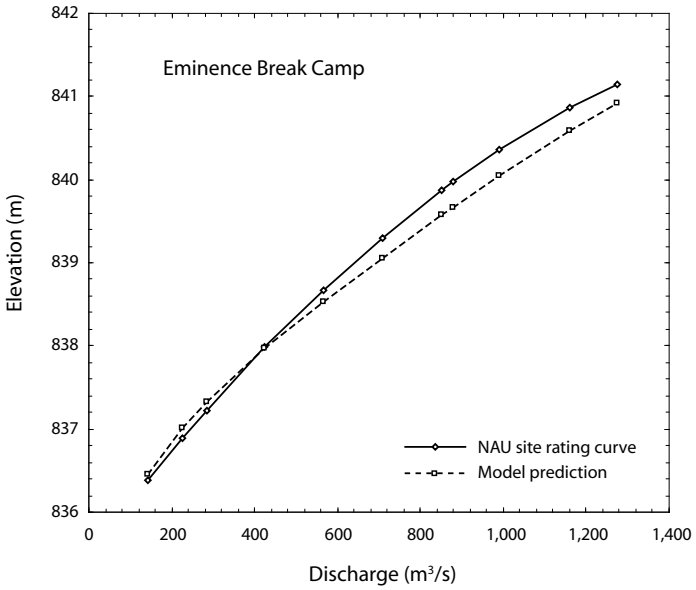

Figure 10. Comparison of the hydraulic model predictions and the stage-discharge data as measured by NAU at Eminence Break Camp near river mile 44.5.

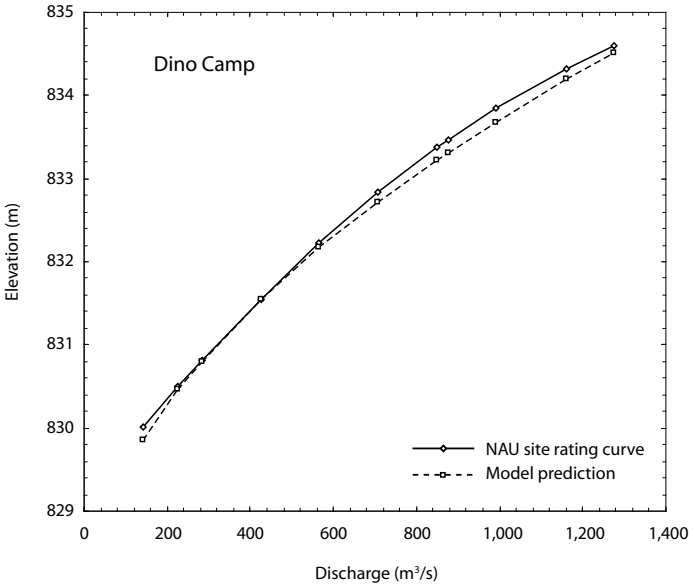

Figure 11. Comparison of the hydraulic model predictions and the stage-discharge data as measured by NAU at Dino Camp near river mile 50.

and with 68% confidence, the hydraulic model predicts stage in the river to within ±0.32 m. The model accuracy was ±0.64 m at 878 m^3/s, when flow begins to inundate the overbank regions. Heavy riparian vegetation on the lower sections of the overbanks results in a larger roughness and a higher water-surface elevation than the model predicts. The model, using a constant 0.035 roughness coefficient, may fail to capture energy losses from extra vegetation on the overbanks. Another potential source of error is recirculation eddies along the river corridor. The presence of eddies, particularly upstream and downstream from debris fans, act to both consume energy in

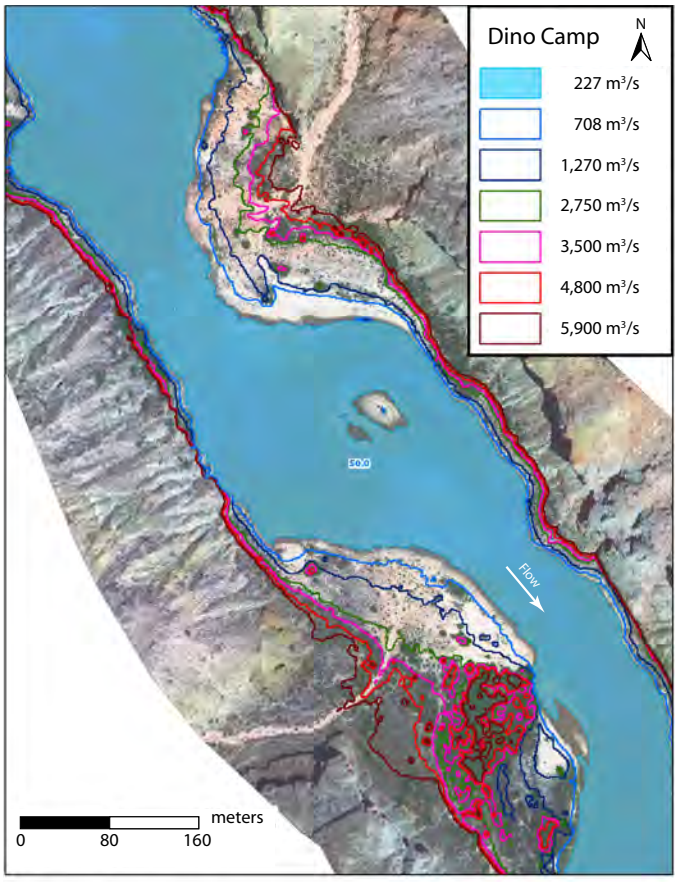

Figure 12. Virtual shorelines at River Mile 50. The effects of the vegetated surface in the DEM can be seen as island polygons.

Table 6. Error measured relative to all NAU monitoring sites at varying discharge with a constant roughness coefficient of n=0.035.

Discharge (m^3/s)	Residual mean (m)	Standard deviation of the residuals (m)	Total estimated error (m)	Percent error
142	-0.03	0.34	0.37	45%
227	0.03	0.30	0.32	25%
283	0.02	0.29	0.30	19%
425	-0.06	0.29	0.35	15%
566	-0.15	0.31	0.46	15%
708	-0.23	0.33	0.56	16%
850	-0.29	0.34	0.63	15%
878	-0.30	0.35	0.64	15%
991	-0.31	0.36	0.67	15%
878	-0.29	0.37	0.66	13%
1,274	-0.24	0.38	0.62	12%

the flow and constrict the conveyance of the channel. Because the hydraulic model is one-dimensional, it cannot account for the recirculation eddies, potentially affecting model accuracy. Also, as the discharge in the Colorado River in Grand Canyon increases from 300 m^3/s up to larger intermediate discharges near 1,000 m^3/s, many rapids wash out (become less steep and experience a reduction in the total elevation drop through the rapid) as downstream features exert hydraulic control over these rapids. In the river, more energy is consumed in strong turbulence within the pools, and less energy is consumed by the constriction of rapids. The hydraulic model, which under subcritical flow regime consumes large amounts of energy in the rapids at low discharge, may potentially under predict the energy consumption in pools, resulting in an under prediction of the stage.

A comparison of the results of the hydraulic model to the stage data reported by Konieczki and others (1997) shows that for a change in discharge from 237 m^3/s to 1,322 m^3/s, the mean of the residuals of the 27 sites indicate the model under predicted stage by -0.14 m. The standard deviation of these residuals is 0.39 m indicating an overall accuracy of ±0.53 m. These error estimates using the data from Konieczki and others is consistent with the accuracy estimates using the NAU data.

To evaluate the sensitivity of the model to different values of Manning's n, global roughness values of 0.025 to 0.045 were evaluated and compared to the standard n=0.035 (fig. 14). At the smallest discharge evaluated, 142 m^3/s, average error changed roughly 0.30 m as roughness is raised from n=0.025 to n=0.045. At the largest discharge, 1,274 m^3/s, average error changed roughly 0.88 m over the span of roughness values evaluated. For flow between 700 and 1,300 m^3/s, figure 14 indicates a global roughness of n=0.040 slightly improves model performance, suggesting the model underestimated energy loss at moderate discharges from either overbank vegetation or larger eddies in the flow.

Modeling Floods between 1,400 and 2,500 m^3/s

The residuals as a function of discharge up to 2,500 m^3/s for the four NAU sites and two USGS gaging stations are shown in figure 15. At 1,700 m^3/s, the residuals and standard deviation from the six sites is 0.12±0.67 m. At 2,500 m^3/s, the mean of the residuals is 0.20±0.76 m giving an overall accuracy of about 1.0 m.

The model agreed well with the two USGS gaging stations with the residuals under 0.5 m. The model also agreed well with the NAU data reported at river mile 220. This NAU rating curve for this site was constructed using high-water marks from the 1983 flood (2,750 m^3/s). Similarly, the rating curve at Vaseys Paradise was constructed with 1983 high-water marks, but the hydraulic model under predicted stage by about one meter. This section of river is in a narrow reach of canyon and the model estimate of n=0.035 may not represent the true energy losses. In contrast, the model tends

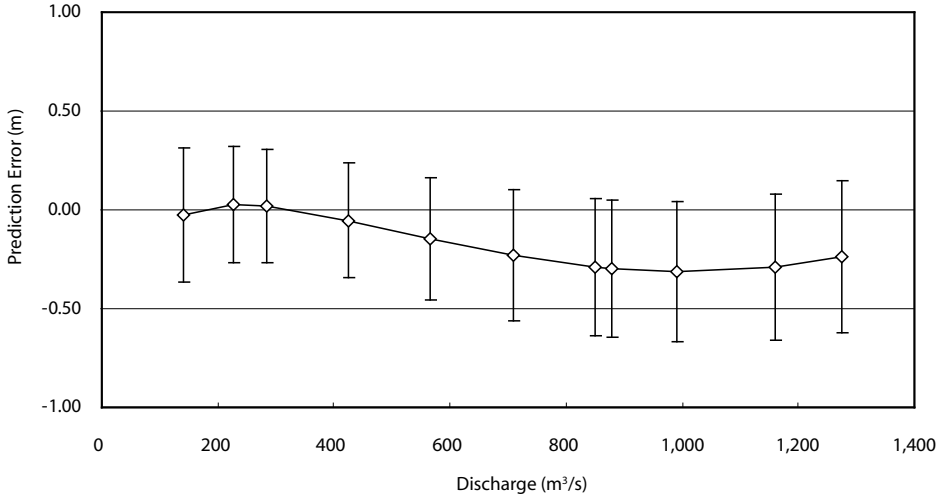

Figure 13. The average of the residuals of the hydraulic model predictions compared against stage-discharge data measured at the NAU monitoring sites. The error bars represent the standard deviation of the residuals.

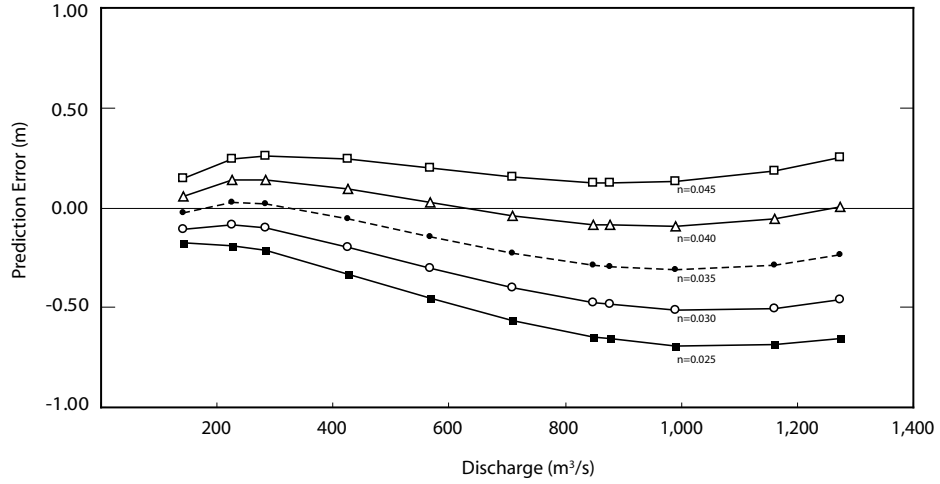

Figure 14. Sensitivity analysis of the model residual mean (averaged for all NAU sites) for different values of Manning's *n*.

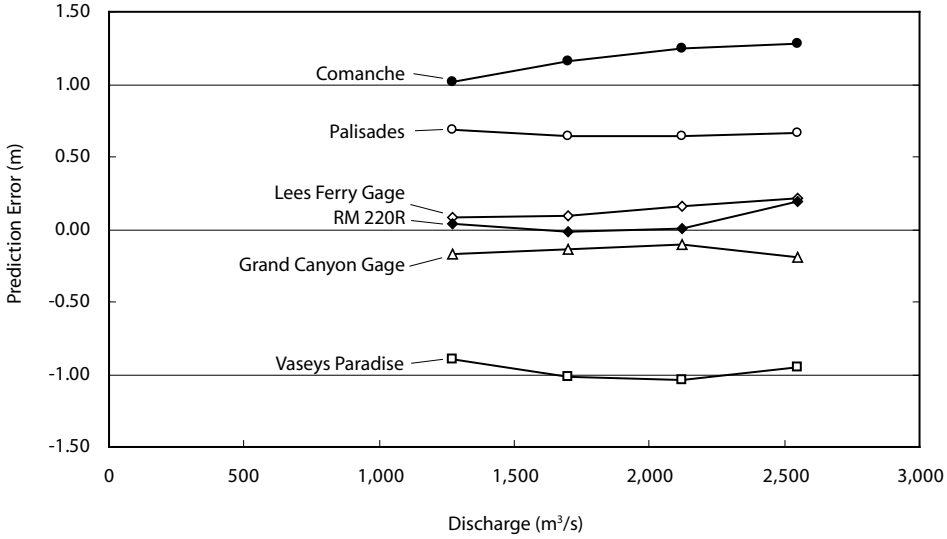

Figure 15. The residual error calculated at six sites for discharges from 1,400 to 2,500 m³/s.

Figure 16. Matched photos showing the section of river at Boulder Narrows (river mile 18.746) during (top) 3,570 m^3/s flood on 6/11/1957 with P.T. Reilly rowing (Duane Norton, NAU.PH.97.46.115.63, courtesy of Northern Arizona University, Cline Library, Special Collections and Archives, P.T. Reilly Collection) and (bottom) low flow of roughly 340 m^3/s photographed 3/1/2005 (Steve Young, Desert Laboratory Repeat Photography Collection, stake 4810).

to over predict stage at the Palisades and Comanche sites. The NAU rating curves above 1,300 m^3/s for these sites were constructed from driftwood data (Draut and others, 2005). It may be that within this geomorphically wide reach of the river, the roughness coefficient needed to model the river is lower than 0.035. The river in Furnace Flats is relatively wide with a lesser gradient than other sections of the river. As the water depth increases with rising stage, roughness elements on the bed become smaller in a relative sense and the overall roughness coefficient, in theory, drops. For example, in Glen Canyon, the Bureau of Reclamation (1957) reported Manning's *n* decreased from 0.03 to 0.02 as flow increased from 283 to 2832 m^3/s. The other possible explanation for the apparent over prediction of stage is that debris flow activity in this reach of the river has significantly aggraded the river bed. For example, at least four debris flows occurred at either Lava Canyon or Palisades Creek (river mile 66.0) between 1965-1984 (Cooley and others, 1977; Melis and others, 1994; Webb and others, 2000), two debris flows occurred at Comanche Creek (river mile 67.7) between 1999-2001, creating a rapid, and one large debris flow occurred at Tanner Creek in 1993 (Melis and others, 1994). These debris flows and associated boulders raised the river. At Tanner Rapid, Melis and others (1994) report a rise of 1.0 m in 1993 that was lowered 0.27 m by a flood in 1996 (Webb and others, 1999). Though the rise in the water-surface elevation at Comanche and at Palisades was not measured, the size and number of debris flows and the observation of a new rapid at Comanche suggest the river also rose in this reach by an amount similar to Tanner Rapids. Because the hydraulic model was built with modern topography, aggraded with fresh debris-flow material, the predicted water surface is probably higher than the water surface 20 years earlier, possibly explaining the over prediction with respect to driftwood strand lines.

Modeling Large Floods

Photographic evidence of historic floods can be used to verify the accuracy of the hydraulic model for large discharges. For example, a photograph taken during the 3,570 m^3/s flood in 1957 shows the water level and P.T. Reilly navigating his boat through Boulder Narrows (river mile 18.746) in Marble Canyon (fig. 16). This 1957 flood was the largest in Grand Canyon in the past 79 years. Boulder Narrows is a well-known section of the Colorado River where a large boulder on the order of 10-20 m fell into the center of the river channel; at low discharge, the river flows to either side of the boulder whereas the boulder is overtopped during large discharge (fig. 16). When this section of the river was simulated with the hydraulic model, the predicted water-surface elevation fell roughly one meter below the top of the boulder (fig. 17). The predicted water surface of the river for a flood of 3,570 m^3/s is just below the top of the boulder at Boulder Narrows, but because the model is one-dimensional, it does not account for localized backwater effects of the flowing water as it backs up

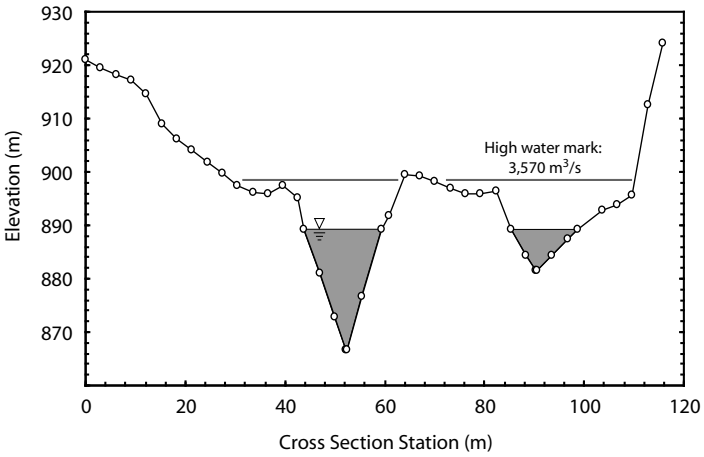

Figure 17. Hydraulic model cross section at river mile 18.746 (Boulder Narrows) showing predicted water-surface elevation at 227 m^3/s (the shaded area) and the predicted high water mark of the 3,570 m^3/s flood that occurred in Grand Canyon in 1957. The peak of the actual flood overtopped the boulder (fig. 14); the model under predicts the stage of the flood high-water mark by about 1 m.

behind the boulder. If the localized backwater effect was considered (for example, in a two-dimensional model) the model would better predict the incipient overtopping of the boulder shown in figure 16. In fact, the elevation of the stage plus the velocity head at this cross section in the model is 0.48 m above the top of the boulder, confirming that with impinging flow, the model does predict the over topping of the boulder.

Driftwood lines from large pre-dam floods are visible today throughout Grand Canyon. Based on the driftwood lines left by large historic floods near Palisades Creek at river mile 66 (David Topping, USGS, written communication, 2005), the hydraulic model over predicted the water-surface elevation in this reach by 1.11 m at 5,000 m^3/s and 1.40 m at 5,900 m^3/s (fig. 18). This over prediction by the model may be related to the choice of a Manning's roughness coefficient that may be too large for this section of the river. The hydraulic conditions of the river, however, have also changed between 1921 and 2000. As mentioned above, high debris-flow activity in this section of the river during the post-dam era has aggraded the river channel. Also important, a significant increase in the quantity of riparian vegetation below the 3,000 m^3/s water line (Webb, 1996; Webb and others, 2007) has changed the roughness elements along the overbanks. With these changes both in vegetation and the topography on debris fan, it is probable that if a flood of 4,800 m^3/s or 5,900 m^3/s came down the river today, the water surface would be higher than high-water marks indicated by the driftwood strand lines left in 1921 and 1884, though that rise might not be as great as 1.11 m or 1.40 m.

More recently, numerous driftwood strand lines and driftwood piles were left throughout the river corridor from the 3,570 m^3/s flood in 1957. Granite Park, located near river mile 209, is a relatively wide expanse of river corridor caused by faulting of the Granite Park Fault (fig. 19). Just upstream of

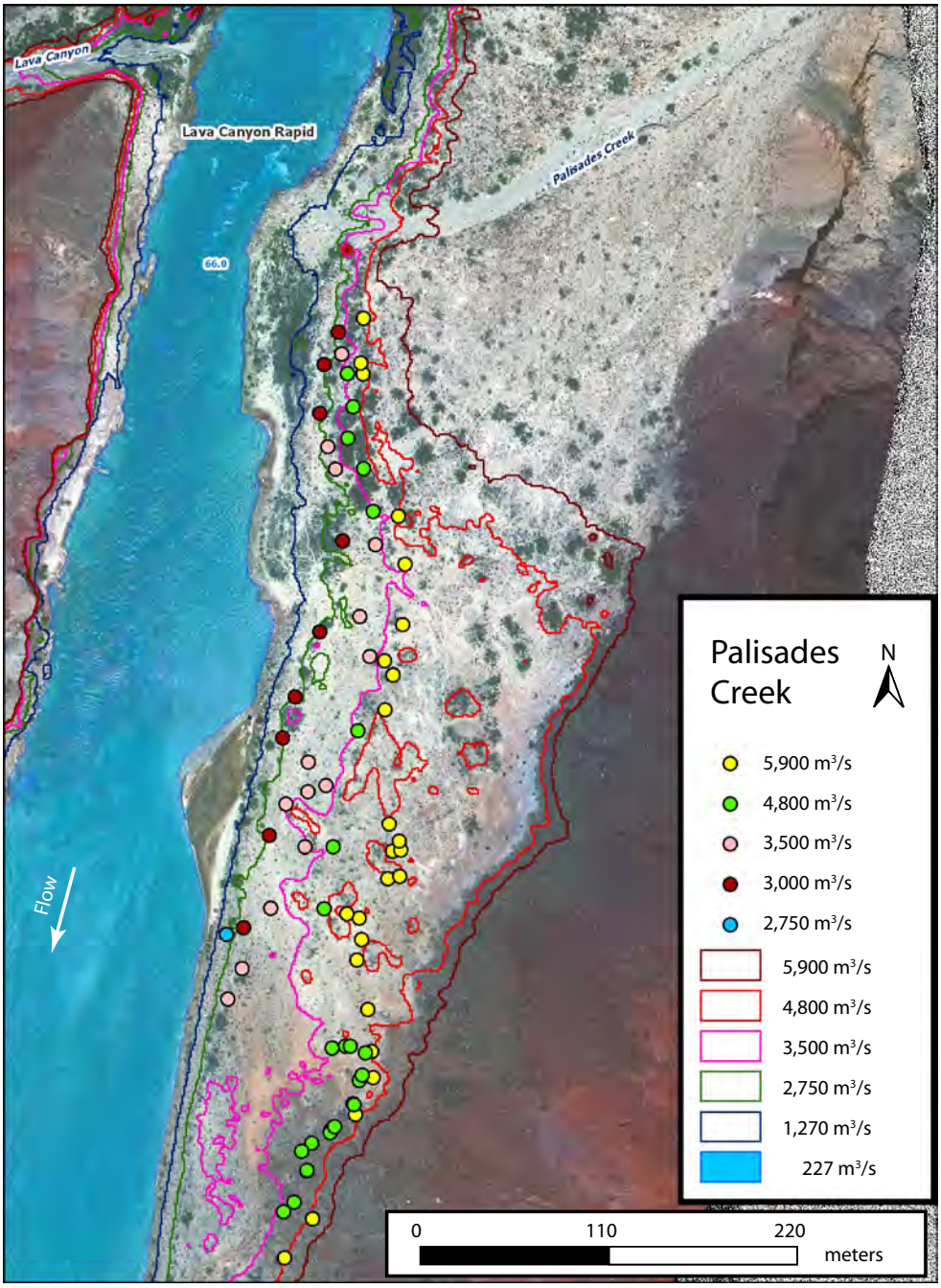

Figure 18. Virtual shorelines (shown as lines) and driftwood strands (shown as dots) for different floods at Palisades Creek (river mile 66) generated with a Manning's n value of 0.035. The results indicate that for this section of river, the model over predicts the water-surface elevation for flows above 4,800 m^3/s by as much as 1.4 m.

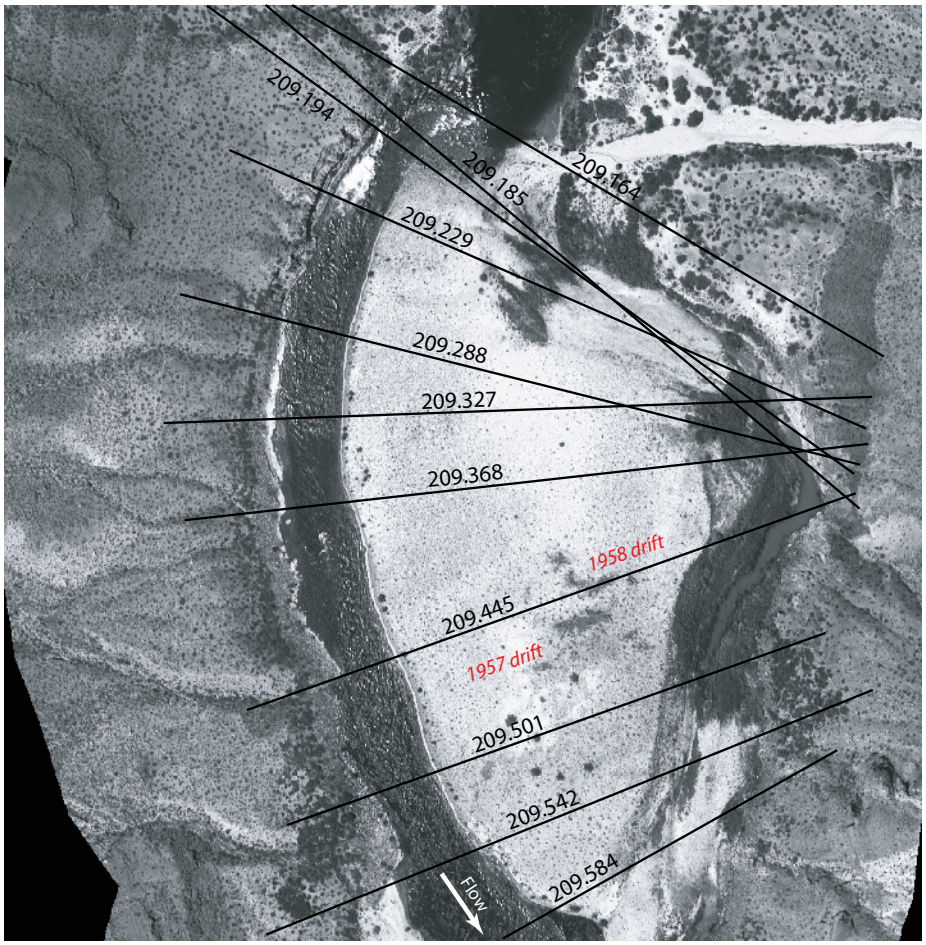

Figure 19. Reach of river in Granite Park (river mile 209) showing the broad boulder bar formed from reworked particles entering from the tributary on river left. The flow of the river in the image is from top to bottom. Collections of driftwood left by the 1958 (3,000 m^3/s) flood and the 1957 (3,570 m^3/s) flood are visible toward the middle of the boulder bar near cross section 209.445; these two driftwood piles are labeled.

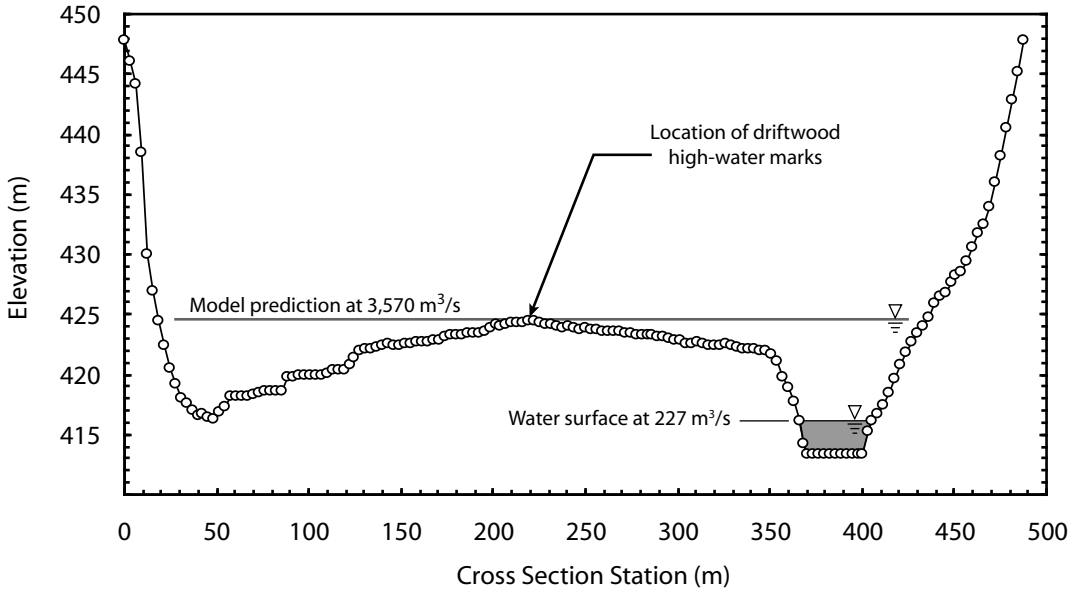

Figure 20. Hydraulic model prediction of the water-surface elevation at river mile 209.445. The inundation of 227 m^3/s is shown as the gray area. The high water mark of the 1957 flood (3,570 m^3/s) is also shown illustrating the prediction accuracy for high discharges for this reach of river.

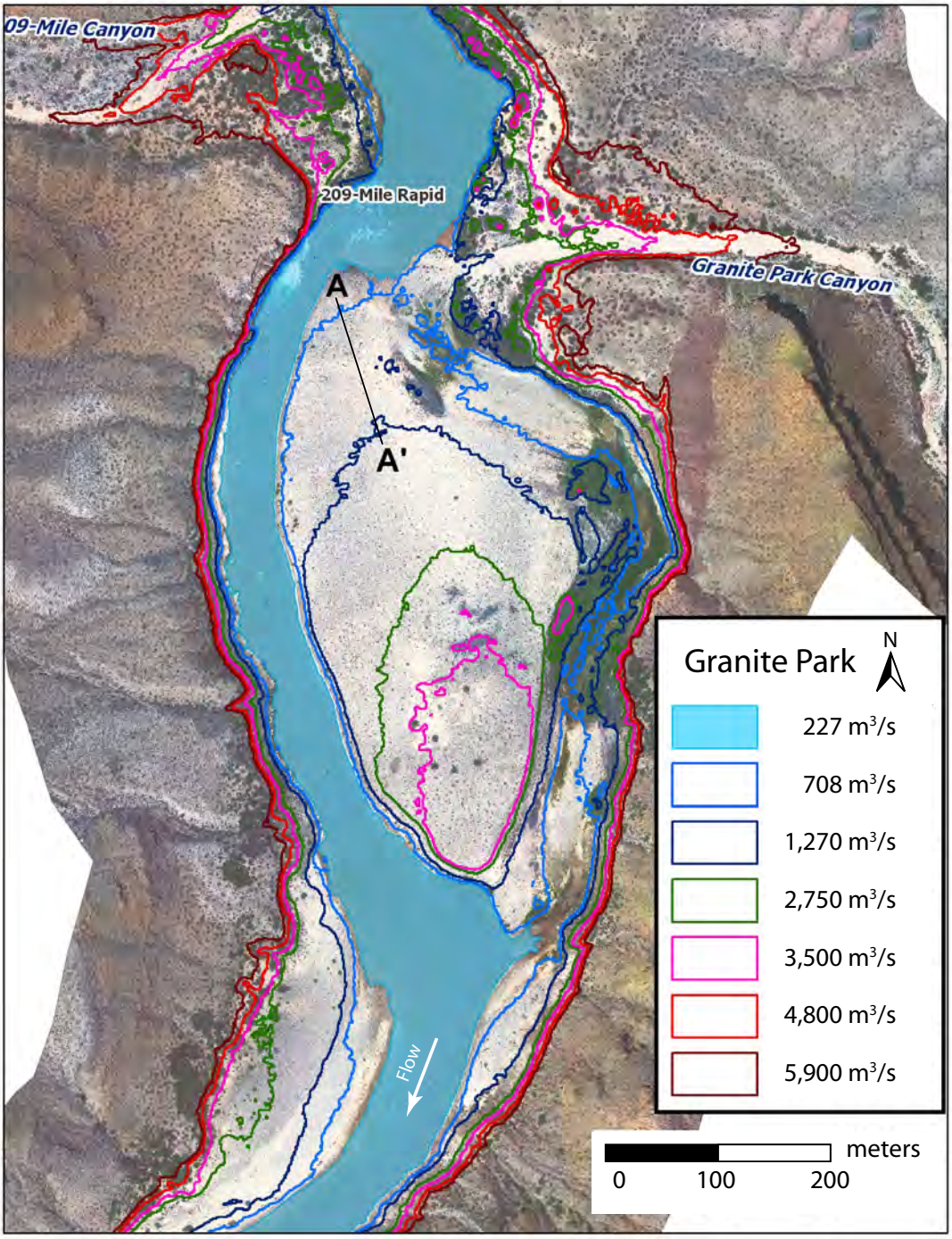

Figure 21. Virtual shorelines at Granite Park (river mile 209) as predicted by the hydraulic model. The line A-A' extends between the 708 and 1,274 m^3/s shorelines and rises 1.9 meters across a distance of 100 meters.

the expansion, three closely spaced tributaries dump coarse-grained sediment into the river that has been reworked into a large boulder-strewn island, which rises in elevation in the downstream direction. At low flows, the river flows entirely around the right edge of the island. With increasing discharge, the river flows around the island with its highest point at the farthest downstream point of the bar. Extremely large flows (greater than 5,500 m^3/s) completely submerge the island. The floods of 1957 (3,570 m^3/s) and 1958 (3,000 m^3/s) did not overtop the bar and left large driftwood piles in the lower middle section of the island. The dark gray splotches shown on figure 19 at cross section 209.445 is the 1958 driftwood pile and the larger gray splotch just downstream is the 1957 driftwood pile (David Topping, USGS, written communication, 2008). In the hydraulic model for 3,750 m^3/s, the cross section at river mile 209.368 was completely submerged while the cross section at river mile 209.501 still showed a prominent island. The predicted water surface just touched the top of the boulder bar at cross section 209.445 (fig. 20), roughly predicting the location of the driftwood piles left in 1957.

Mapping the virtual shorelines is useful at Granite Park, with the presence of the wide, flat boulder bar. Figure 21 show various inundation shorelines at Granite Park from 227 m^3/s up to 5,900 m^3/s. The horizontal accuracy of virtual shoreline placement in the inundation maps was affected by three factors, (1) the vertical accuracy of the stage at any given cross section, (2) the error associated with bare-ground elevations contained within the DEM, and (3) the slope of the ground surface across any area of interest. This last factor is of particular concern since relatively small vertical discrepancies can result in sizeable line-placement differences across surfaces of low slope, as seen at Granite Park between the 708 and 1,274 m^3/s shorelines. Here, there is a 1.9 m vertical stage difference between the two shorelines, but the horizontal distance, from north to south, is at least 100 m. Thus, when horizontal placement accuracy of the shoreline is an issue, care should be taken in evaluating the stage-discharge relation at the particular location.

To more rigorously test the predictive accuracy of the hydraulic model for large floods, model results were compared to the stage-discharge relations established at the USGS gaging stations at Lees Ferry and Grand Canyon. Comparison of the model results with data from the gaging station at Grand Canyon shows how well the model accurately predicts stage (fig. 22). Up to 2,500 m^3/s, the prediction error is less than -0.20 m. The greatest prediction error -0.34 m occurs for flows between 3,000-5,000 m^3/s, representing a percentage error of 4%. The error at 5,900 m^3/s is -0.23 m. To test if other roughness values may give better results for large floods, the model was run with higher Manning's *n* (fig. 22). For the gage at Grand Canyon, it appears that a Manning's *n* value of 0.040 would better predict the water-surface elevation for floods approaching 5,900 m^3/s, with an error of 0.07 m. This observation runs counter to speculation that for deeper flow depths, the relative size of roughness elements in the channel would decrease and the model would require smaller roughness to accurately predict the water surface. The gaging station at Grand Canyon is in Upper Granite Gorge. This reach has a narrow, confined bedrock corridor. The overall channel slope is also relatively steep in this section of river (Hanks and Webb, 2006). As stage rises with discharge near this gaging station, the river appears to expend energy both from flowing against the narrow bedrock walls and from enhanced energy consumption in the narrow gorge resulting from turbulent eddies and waves breaking on the water surface.

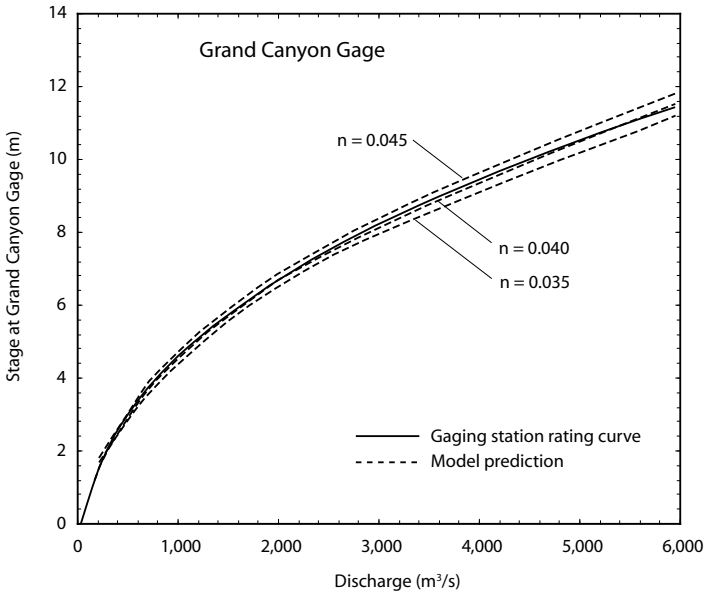

Figure 22. The stage-discharge curve for the gaging station for Colorado River near Grand Canyon, Arizona (09402500) compared to the predicted stage-discharge curves from the hydraulic model for *n*=0.035, *n*=0.040, and *n*=0.045 (gage data taken from Topping and others, 2003). At a discharge of 5,900 m^3/s, the difference in stage between the rating curve and model prediction for *n*=0.035 is -0.23 m. For this location, a roughness value of *n*=0.040 seems to be the best value for model prediction.

At the Lees Ferry gage, the hydraulic model accuracy was good for smaller flows, but the model tended to over predict the water-surface elevation for discharge above 2,000 m^3/s (fig. 23). The model prediction error was generally less than 0.10 m at discharges less than 2,000 m^3/s. Error steadily increased with discharge, reaching a value of 0.69 m at 5,900 m^3/s. When a roughness sensitivity analysis was performed, the model accuracy improved if the Manning's *n* value was decreased to 0.030 for a discharge above 4,000 m^3/s, but the overall model accuracy for flows between 2,000 and 4,000 m^3/s was about equivalent for roughness values of 0.030 and 0.035 (fig. 23).

Though independent stage-discharge relations for high discharge were only available at these two long-term gaging stations, the results of the analysis suggest that model accuracy is generally within 1.0 m for discharges up to 5,900 m^3/s. The model appears to better predict stage in narrow, confined sections of the river though more analysis is needed to fully evaluate the model's performance in geomorphically wide sec-

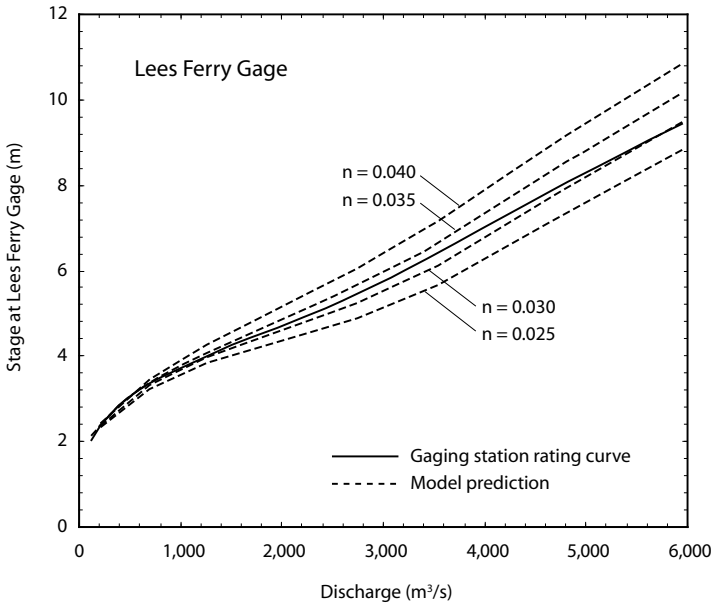

Figure 23. The stage-discharge curve for the gaging station for Colorado River at Lees Ferry, Arizona (09380000) compared to the predicted stage-discharge curve from the hydraulic model for *n*=0.025, *n*=0.030, *n*=0.035, and *n*=0.040 (gage data taken from Topping and others, 2003). At a discharge of 5,900 m³/s, the difference in stage between the rating curve and model prediction for *n*=0.035 is 0.69 m. For this location, a roughness value of *n*=0.030 seems to be the best value for model prediction.

Table 7. Error measured relative to all NAU monitoring sites for discharge up to 1,274 m³/s with the recommended roughness coefficients.

Discharge (m³/s)	Recommended Manning's n	Residual Mean (m)	Standard deviation of the residuals (m)	Percent Error
142	0.037	0.00	0.34	42%
227	0.034	0.01	0.29	23%
283	0.034	-0.01	0.28	18%
425	0.037	0.00	0.29	12%
566	0.039	-0.01	0.31	11%
708	0.041	0.00	0.34	9%
850	0.042	0.00	0.36	9%
878	0.042	0.00	0.36	9%
991	0.042	0.00	0.38	8%
1,161	0.041	-0.01	0.38	8%
1,274	0.040	0.00	0.39	7%

tions of the river (for example, Furnace Flats near river mile 68).

The hypothesis that smaller Manning's n value would be needed to accurately model large floods may be valid in some sections of the river, but the overall set of evidence suggests the choice of Manning's n of 0.035 is largely appropriate for most sites even at large discharge. While a slightly lower roughness coefficient at Lees Ferry was justified, data from the gaging station near Grand Canyon suggest that larger Manning's n values for extreme flows are also justified. For geomorphically wide reaches, a lower Manning's n value is justified for limited cases. Moreover, the qualitative data from Palisades suggest a low roughness value may be needed in the wide geomorphic reach of Furnace Flats (near river mile 68), but in western Grand Canyon, data from Granite Park—also located in a geomorphically wide reach—indicate that a Manning's n of 0.035 is appropriate. The specific results at Palisades may be explained by changes in the hydraulic conditions along the river corridor or the two-dimensional nature of the recirculation eddy below the rapid which cannot be modeled accurately by the one-dimensional hydraulic model. Looking at the overall results of the study, a Manning's n value of 0.035 is probably the best roughness coefficient overall for the Colorado River Grand Canyon.

Suggested roughness values for flows below 1,400 m³/s

All flows in the Colorado River in Grand Canyon since 1987 have been below 1,400 m³/s. With the quality of stage-discharge data collected by NAU, the roughness values in the channel and overbanks used when running the final, calibrated model can be adjusted to improve the accuracy of the model for these smaller flows. (While the synthetic bathymetry of the model was initially calibrated using a Manning's n of 0.035, the final model can be easily run using any specified roughness value.) Using these NAU data, recommended values of Manning's roughness coefficient were determined for selected flows up to 1,274 m³/s (table 7). Also, figure 24 shows the mean and the standard deviation of the residuals for each of the flows listed in table 7. Using these adjusted roughness values, the accuracy of the model is better than 0.40 m for all discharges below 1,400 m³/s.

Future Model Adaptations

The hydraulic model built for Grand Canyon is useful and reasonably predicts flow up to 5,900 m³/s. As discussed throughout this report, however, there are opportunities to improve the model. Cross sections in wide or strongly sinuous sections of the river could be regenerated into broken segments to better model flow perpendicular to each cross section, taking care that adjacent cross sections do not intersect. The roughness coefficient at each cross section can be better

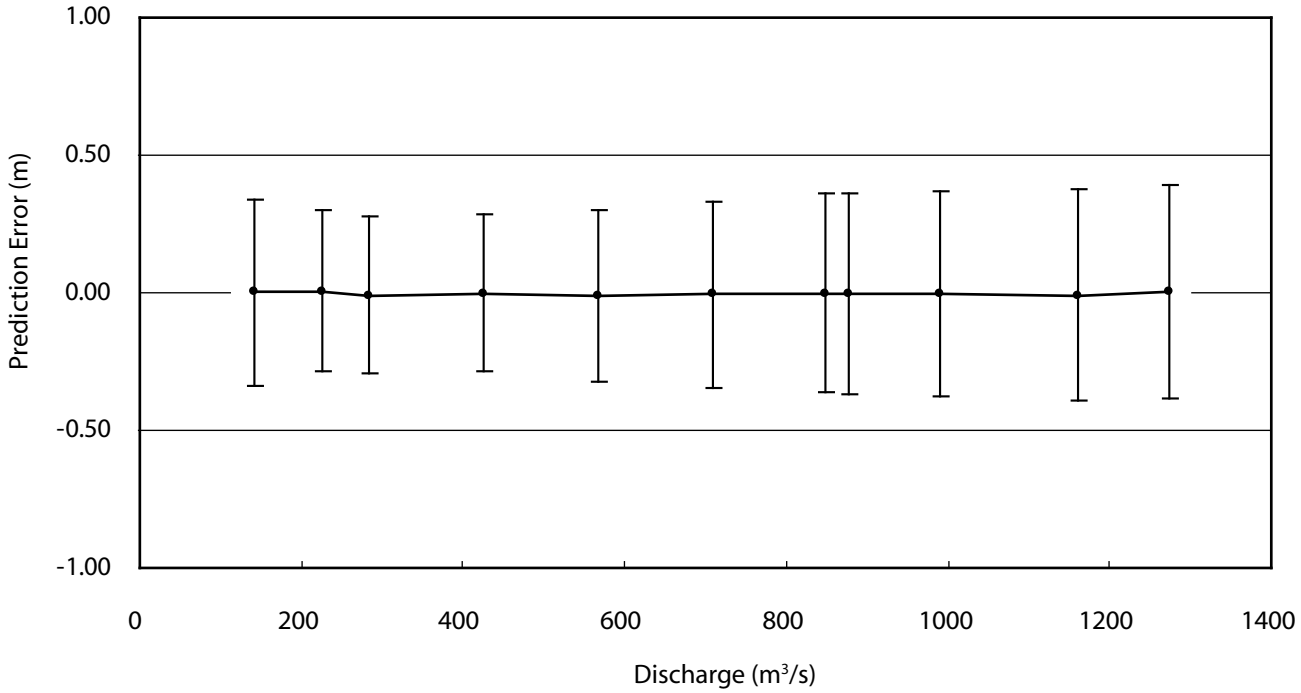

Figure 24. The average of the residuals of the hydraulic model predictions compared against stage-discharge data measured at the NAU monitoring sites when then Manning's roughness coefficient has been tuned to produce optimal model results. The error bars represent the standard deviation of the residuals.

estimated based on local conditions in the channel and the overbanks. The roughness coefficient could also vary as a function of discharge and reach type (that is, narrow versus wide). Based on the results of the analysis of the synthetic bathymetry, a larger Manning's *n* value in the channel could have enabled the synthetic bathymetry to more closely match the real bathymetry. The model's relative accuracy above 227 m^3/s suggests, however, that if a larger Manning's *n* was used to create synthetic bathymetry, smaller roughness values would be needed for larger discharges and in the overbank regions, greatly increasing the complexity of the model. As it becomes available, real bathymetry measured from the river can be incorporated into the model. If significant debris flows impact the river in the future, the synthetic bathymetry at the location of the debris flow can be updated to capture changes to the water-surface profile. Instead of using universal values for expansion and contraction coefficients, the coefficients at each cross section could be tailored to match the hydraulic conditions for that location. And finally, HEC-RAS has options to insert areas of ineffective flow into the model. To better capture the hydraulic behavior below debris-fan or bedrock constrictions, ineffective flow regions could be placed in the locations of the recirculation eddies.

Conclusions

A hydraulic model using GIS-based techniques to visualize shoreline inundation was constructed for 364 km of the Colorado River in Grand Canyon. The model simulates flood events up to 5,900 m^3/s using 2,680 cross sections. The model was built using topography collected in 2000 and 2002, and the model was built in HEC-RAS. The GIS-based techniques take the output of the hydraulic model and map inundation along the river corridor for any location between Lees Ferry and Diamond Creek.

Based on independently collected stage-discharge data from NAU and the USGS, the total error of predicted water-surface elevations from the model is about 0.30 m for flows less than 425 m^3/s. For flows between 425-1,300 m^3/s, error is about 0.40 m using the recommended roughness coefficients. For flows between 1,300-2,500 m^3/s, error is about 1.0 m. For floods up to 5,900 m^3/s, the model is a reasonable predictor of stage with an error of about 1.5 m (roughly 15%). Anecdotal analyses of the 1957 flood deposits at Boulder Narrows and Granite Park show that the model produces a comparable stage and appears to reasonably predict large flows in confined or narrow river reaches while possibly over predicting stage in wide reaches of the river corridor.

Finally, the approach of generating synthetic bathymetry in the place of actual bathymetry when actual bathymetry is difficult to obtain is both unique and unorthodox. Analyses in this report show that while the approach can produce a useful model, the careful choice of roughness coefficient before calibrating the synthetic bathymetry can improve the value of the model by enabling a more accurate guess of the true bathymetry.

References Cited

Bathurst, J.C., 2002, At-a-site variation and minimum flow resistance from mountain rivers, Journal of Hydrology, Vol. 269, p. 11-26.

Bennett, J.P., 1993, Sediment Transport Simulations for Two Reaches of the Colorado River, Grand Canyon, Arizona: U.S. Geological Survey Water-Resources Investigations Report 93-4034, 42 p.

Benson, M.A. and T. Dalrymple, 1967, General field and office procedures for indirect discharge measurements, U.S. Geological Survey Techniques in Water Resources Investigations, Book 3, Chapter A1, 30 p.

Brunner, G.W., 2002, HEC-RAS river analysis system: hydraulic reference manual, version 3.1: Davis, California, U.S. Army Corps of Engineers, Institute for Water Resources, Hydrologic Engineering Center.

Bureau of Reclamation, 1957, Tail water and degradation studies, Colorado River below Glen Canyon Dam, U.S. Bureau of Reclamation, Denver, Colorado, 10 p.

Bureau of Reclamation, 1996, Environmental assessment on the experimental flood: Glen Canyon Dam. Bureau of Reclamation, Salt Lake City, Utah.

Bureau of Reclamation, 2001, Josephine County Water Management Improvement Study, Oregon: Savage Rapids Dam Sediment Evaluation Study, Department of the Interior, 284 p.

Chow, V.T., 1959, Open channel hydraulics: New York, McGraw Hill, 680 p.

Cooley, M.E., B.N. Aldridge, and R.C. Euler, 1977, Effects of the catastrophic flood of December, 1966, North Rim area, eastern Grand Canyon, Arizona, U.S. Geological Survey Professional Paper 980, 43 p.

Davidian, J., 1984, Computation of water-surface profiles in open channels: U.S. Geological Survey Techniques in Water Resources Investigations, Book 3, Chapter A14, 48 p.

Draut, A.E., Rubin, D.M. Dierker, J.L., Fairley, H.C., Griffiths, R.E., Hazel, J.E. Jr, Hunter, R.E., Kohl, K., Leap, L.M., Nials, F.L. Topping, D.J. and Yeatts, M. 2005, Sedimentology and Stratigraphy of the Palisades, Lower Comanche, and Arroyo Grande Areas of the Colorado River Corridor, Grand Canyon, Arizona, 2005, U.S. Geological Survey Scientific Investigations Report 2005-5072, 68 p.

Feldman, A.D., 1981, HEC models for water resources system simulation, theory and experience: Advances in Hydroscience, v. 12, p. 297-423.

Flynn, M.E., and Hornewer, N.J., 2003, Variations in Sand Storage Measured at Monumented Cross Sections in the Colorado River Between Glen Canyon Dam and Lava Falls Rapid, Northern Arizona, 1992-99: U.S. Geological Survey Water-Resources Investigations Report 03-4104, 39 p.

Garrett, W.B., Van De Vanter, E.K., and Graf, J.B., 1993, Streamflow and sediment-transport data, Colorado River and three tributaries in Grand Canyon, Arizona, 1983 and 1985-86, U.S. Geological Survey Open-File Report 93-174, 624 p.

Gauger, R.W., 1996, River-Stage Data, Colorado River, Glen Canyon Dam to Upper Lake Mead, Arizona, 1990-94, U.S. Geological Survey Open-File Report 96-626, 20 p.

Graf, J.B., 1995, Measured and predicted velocity and longitudinal dispersion at steady and unsteady flow, Colorado River, Glen Canyon Dam to Lake Mead, Journal of the American Water Resources Association, Vol. 31, No. 2, pp. 265-281, doi:10.1111/j.1752-1688.1995.tb03379.x.

Grand Canyon Monitoring and Research Center, 2002, A guide to the Colorado River in the Grand Canyon: From Glen Canyon Dam to Pierce Ferry: Flagstaff, Arizona, U.S. Geological Survey, Grand Canyon Monitoring and Research Center.

Grant, G.E., 1997, Critical flow constraints flow hydraulics in mobile-bed streams: A new hypothesis, Water Resour. Res., v. 33 no. 2, p. 349-358.

Griffiths, P.G., R.H. Webb, and T.S. Melis, 2004, Frequency and initiation of debris flows in Grand Canyon, Arizona, Journal of Geophysical Research, v. 109, F04002, doi: 10.1029/2003JF000077.

Hanks, T.C. and R.H. Webb, 2006, Effects of tributary debris on the longitudinal profile of the Colorado River in Grand Canyon, Journal of Geophysical Research, v. 111, F02020, doi:10.1029/2004JF000257.

Hazel, J.E. Jr, Kaplinski, M., Parnell, R. Kohl, K., and Topping, D.J., 2007, Stage-Discharge Relations for the Colorado River in Glen, Marble, and Grand Canyon, Arizona, 1990-2005, U.S. Geological Survey Open-File Report 2006-1243, 7 p.

Henderson, F.M., 1966, Open channel flow: New York, MacMillan, 522 p.

Hoggan, D.H., 1997, Computer-assisted floodplain hydrology and hydraulics: New York, McGraw-Hill, 676 p.

Howard, A., and Dolan, R., 1981, Geomorphology of the Colorado River in Grand Canyon: Journal of Geology, v. 89, p. 269-298.

Jarrett, R.D., 1984, Hydraulics of high-gradient streams: Journal of the Hydraulics Division, American Society of Civil Engineers, v. 110, no. 11, p. 1519-1539.

Kidson, R.L., Richards, K.S. and Carling, P.A., 2006, Hydraulic model calibration for extreme floods in bedrock-confined channels: case study from northern Thailand, Hydrologic Processes, v. 20, p. 329-344, doi:10.1002/hyd.6086.

Kieffer, S.W., 1985, The 1983 hydraulic jump in Crystal Rapid: Implications for river-running and geomorphic evolution in the Grand Canyon, Journal of Geology, v. 93, p. 385-406.

Konieczki, A.D., Graf, J.B., and Carpenter, M.C., 1997, Streamflow and sediment data collected to determine the effects of a controlled flood in March and April 1996 on the Colorado River between Lees Ferry and Diamond Creek, Arizona, U.S. Geological Survey Open-File Report 97-224, 55 p.

Leopold, L.B., 1969, The rapids and the pools—Grand Canyon, p. 131-145 in The Colorado River Region and John Wesley Powell, U.S. Geological Survey Professional Paper 669.

Limerinos, J.T., 1970, Determination of the Manning coefficient from measured bed roughness in natural channels, U.S. Geological Survey Water Supply Paper 1898-B, 47 p.

Magirl, C.S., Webb, R.H., and Griffiths, P.G., 2005, Changes in the water surface profile of the Colorado River in Grand Canyon, Arizona, between 1923 and 2000: Water Resources Research, v. 41, W05021, doi:10.1029/2003WR002519.

Magirl, C.S., 2006, Bedrock-controlled fluvial geomorphology and the hydraulics of rapids on the Colorado River, Ph.D. dissertation, Univ. of Ariz., Tucson.

Melis, T.S., R.H. Webb, P.G. Griffiths, and T.J. Wise, 1994, Magnitude and frequency data for historic debris flows in Grand Canyon National Park and vicinity, Arizona, U.S. Geological Survey Water Resources Investigations Report 94-4214. 285 p.

Miller, A.J. and B.L. Cluer, 1998, Modeling considerations for simulation of flow in bedrock, *in* Rivers Over Rock: Fluvial Processes in Bedrock Channels, Keith J. Tinkler and Ellen E. Wohl (editors) AGU Monograph 107, AGU, Washington, p. 61-103.

O'Conner, J.E. and Webb, R.H., 1988, Hydraulic modeling for paleoflood analysis, in Flood Geomorphology, Baker, V.R. Kochel, R.C., and Patton, P.C. (editors), Wiley, New York, p. 393-402.

O'Connor, J.E., Ely, L.L., Wohl, E.E., Stevens, L.E., Melis, T.S., Kale, V.S. and Baker, V.R., 1994, A 4500-year record of large floods on the Colorado River in the Grand Canyon, Arizona: Journal of Geology, v. 102, p. 1-9.

Randle, T.J., and Pemberton, E.L., 1987, Results and analysis of STARS modeling efforts of the Colorado River in Grand Canyon: Flagstaff, Arizona, Glen Canyon Environmental Studies, NTIS Report PB88-183421.

Rote, J.J., Flynn, M.E., and Bills, D.J., 1997, Hydrologic data, Colorado River and major tributaries, Glen Canyon Dam to Diamond Creek, Arizona, water years 1990-95, U.S. Geological Survey Open-File Report 97-250, 474 p.

Rouse, H., 1965, Critical analysis of open-channel resistance, Journal of the Hydraulics Division, American Society of Civil Engineers, v. 91(HY4), p. 1-25.

Schmidt, J.C. and J.B. Graf, 1990, Aggradation and degradation of alluvial sand deposits, 1965 to 1986, Colorado River, Grand Canyon National Park, Arizona, U.S. Geological Survey Professional Paper 1493, 74 p.

Schmidt, J.C. and D.M. Rubin, 1995, Regulated streamflow, fine-grained deposits, and effective discharge in canyons with abundant debris fans, in Natural and anthropogenic influences in fluvial geomorphology, edited by J.E. Costa and others, p. 177-195, AGU, Geophysical Monograph 89, Washington, DC.

Shearman, J.O., Kirby, W.H., Schneider, V.R., and Flippo, H.N., 1986, Bridge waterways analysis model, Research Report, Federal Highway Administration, Report Number FHWA/RD-86/108, U.S. Department of Transportation, Washington, D.C., 112 p.

Topping, D.J., Rubin, D.M., and Vierra, L.E. Jr., 2000, Colorado River sediment transport. 1. Natural sediment supply limitation and the influence of Glen Canyon Dam: Water Resources Research, v. 36, no. 2, p. 515-542.

Topping, D.J., Schmidt, J.C., and Vierra, L.E. Jr., 2003, Computation and Analysis of the Instantaneous-Discharge Record for the Colorado River at Lees Ferry, Arizona—May 8, 1921, through September 30, 2000, U.S. Geological Survey Professional Paper 1677, 118 p.

Trieste, D.J., 1992, Evaluation of supercritical/subcritical flows in high-gradient channels: Journal of Hydraulic Engineering, v. 118, no. 8, p. 1107-1118.

U.S. Department of Interior, 1995, Operation of Glen Canyon Dam: Final environmental impact statement, Colorado River Storage Project, Coconino County, Arizona, report, Salt Lake City, Utah, 337 p.

U.S. Geological Survey, 1924, Plan And Profile of Colorado River From Lees Ferry, Ariz., to Black Canyon, Ariz.- Nev. and Virgin River, Nev., U.S. Geological Survey.

Walters, C., Korman, J., Stevens, L.E., and Gold, B., 2000, Ecosystem modeling for evaluation of adaptive management policies in the Grand Canyon: Conservation Ecology, v. 4, no. 2: 1. [online] URL: *http://www.consecol.org/vol4/iss2/art1/*

Webb, R.H., 1996, Grand Canyon, a Century of Change, University of Arizona Press, Tucson.

Webb, R.H., P.T. Pringle, and G.R. Rink, 1989, Debris flows from tributaries of the Colorado River, Grand Canyon National Park, Arizona, U.S. Geological Survey Professional Paper 1492.

Webb, R.H., T.S. Melis, P.G. Griffiths, and J.G. Elliot, 1999, Reworking of aggraded debris fans, in Webb, R.H., J.C. Schmidt, G.R. Marzolf, and R.A. Valdez, (editors), The Controlled Flood in Grand Canyon, Geophys. Mono. 110, p. 37-51 American Geophysical Union, Washington, D.C.

Webb, R.H., P.G. Griffiths, T.S. Melis, and D.R. Hartley, 2000, Sediment delivery by ungaged tributaries of the Colorado River in Grand Canyon, U.S. Geological Survey Water-Resources Investigations Report 00-4055, 67 p.

Webb, R.H. and R.D. Jarrett, 2002, One-dimensional estimation techniques for discharges of paleofloods and historical floods, in Ancient Floods, Modern Hazards, House, K.P., Webb, R.H., Baker, V.R., and Levish, D.R. (editors), The AGU, Washington, D.C. p. 111-125.

Webb, R.H., S.A. Leake, and R.M. Turner, 2007, The Ribbon of Green, Change in Riparian Vegetation in the Southwestern United States, University of Arizona Press, Tucson.

Wiele, S.M., 1997, Modeling of flood-deposited sand distribution in a reach of the Colorado River below the Little Colorado River, Grand Canyon, Arizona, U.S. Geological Survey Water-Resources Investigations Report 97-4168, 15 p.

Wiele, S.M., J.B. Graf, and J.D. Smith, 1996, Sand deposition in the Colorado River in the Grand Canyon from flooding of the Little Colorado River, Water Resources Research, v. 32, no. 12, p. 3579-3596.

Wiele, S.M. and Smith, J.D., 1996, A reach-averaged model of diurnal discharge wave propagation down the Colorado River through the Grand Canyon: Water Resources Research, v. 32, no. 5, p. 1375-1386.

Wiele, S.M. and Griffin, E.R., 1997, Modifications to a one-dimensional model of unsteady flow in the Colorado River through the Grand Canyon: U.S. Geological Survey Water-Resources Investigations Report 97-4046, 17 p.

Wiele, S.M. and M. Torizzo, 2003, A stage-normalized function for the synthesis of stage-discharge relations for the Colorado River in Grand Canyon, Arizona, U.S. Geological Survey Water-Resources Investigations Report 03-4037, 23 p.

Wiele, S.M., Wilcock, P.R., and P.E. Grams, 2007, Reach-averaged sediment routing model of a canyon river, Water Resources Research, v. 43, W02425, doi:10.1029/2005WR004824.

Wilson, 1986, Sonar patterns of Colorado River bed, Grand Canyon, *in* Proceedings of the Fourth Interagency Sedimentation Conference, Subcommittee of Sedimentation of the Interagency Advisory Commission on Water Data, Washington, D.C., v. 2, p. 133-142.

Yen, B.C., 2002, Open channel flow resistance, Journal of Hydraulic Engineering, v. 128, no. 1, p. 20-39, doi:10.1061/(ASCE)0733-9429(2002)128:1(20).